Figure 3. Inhibiting EBV BART miRNA levels affect NKTCL growth rate without affecting cell viability. (**A**) SNK6 cells were transfected with antisense to the indicated EBV miRNAs and cell numbers counted every 24 hours for three days. Cell growth rate was calculated as difference in cell numbers between the 24 hour and 72 hour time point and compared with cells transfected with control Scramble miRNA. Data shown are the average ± SD from three independent experiments. (* represents p value of ≤0.05 in a paired t-test). (**B**) SNK6 transfected with antisense EBV miRNAs were analyzed for viability by Trypan blue exclusion in a Vi-CELL counter every 24 hours for three days. The data presented is the cell viability at 72 hours post-transfection and is the average ± SD from three independent experiments. (**C**) SNT16 cells were transfected with antisense to the indicated EBV miRNAs and cell growth rate analyzed as described above. Data shown are the average ± SD from three independent experiments. (* represents p value of <0.05 in a paired t-test).
doi:10.1371/journal.pone.0027271.g003

Penicillin-Streptomycin and 250 ng/ml Fungizone (Amphotericin B; Invitrogen) and 600 IU of IL-2.

MiRNA microarray analysis and validation

Total RNA was isolated from SNK6 and SNT16 cells using the miRNAeasy kit (Qiagen) as per manufacturer's protocol. RNA was analyzed by LC Sciences (Houston, TX) with miRNA microarrays using the μParaflo microfluidic chip technology and all data is MIAME compliant. The detailed process can be found at http://www.lcsciences.com. Briefly, photogenerated reagent chemistry probes for miRNAs were *in situ* synthesized on chips with three repeats for each probe to allow for statistical analysis. MiRHumanViruses version 13 arrays were used to detect a total of 1100 unique mature miRNAs comprising of 875 human miRNAs and 225 virus miRNAs. The virus miRNAs included 44 EBV miRNAs. RNA samples from SNK6 and SNT16 cells were labeled with Cy3 for hybridization. The chips included 50 control probes based on Sanger miRBase Release 13 with four-sixteen repeats. The control probes were used for quality controls of chip production, sample labeling and assay conditions. Included in the control probes were PUC2PM-20B and PUC2MM-20B which are the perfect match and single-base match detection probes, respectively, of a 20-mer RNA positive control sequence that is spiked into the RNA samples before labeling. For a transcript to be listed as detectable three conditions had to be met: (1) signal intensity had to be greater than three times background standard deviation; (2) spot co-variance (CV), defined as ratio of standard deviation over signal intensity had to be less than 0.5; (3) the signals from at least 50% of the repeating probes had to be above detection level. Data was normalized using a cyclic LOWESS (Locally-weighted Regression) method [45] to remove system related variations such as sample amount variations, dye labeling bias, and signal gain differences between scanners to reveal biological relevant variations. A t-test was performed on the signals obtained for the repeating probes and p-value calculated. MiRNAs were defined as differentially expressed if they had a p-value<0.01. Clustering analysis was performed with a hierarchical method using average linkage and Euclidean distance metric. The clustering data was represented as a heat map using TIGR MeV (Multiple Experimental Viewer; The Institute for Genomic Research). The microarray data has been deposited in GEO database with accession number GSE30695.

Validation of miRNA microarray

Selected EBV miRNAs were quantified using a PCR protocol described by Chen *et al* [46] for detecting miRNAs. Briefly, stem-loop primers complementary to specific EBV miRNAs were designed as described by Cosmopoulos *et al* [19]. For each miRNA assayed, 100 ng of total RNA was reverse transcribed using a TaqMan MicroRNA RT kit as described by the manufacturer and a specific stem-loop primer at a final concentration of 50 nM. RNA was prepared using an RNeasy kit (Qiagen) from exponentially growing tissues culture cells. Each 20 ul PCR reaction contained 1 ul of RT product, 1×TaqMan Universal master mix, 1.5 uM forward primer, 0.7 uM reverse primer, and 0.2 uM probe. The reactions were incubated in a 48-well plate at 95°C for 3 min, followed by 40 cycles of 95°C for 15 s and 60°C for 30 s. The copy number of each of the miRNAs was determined by reverse transcription and amplification of synthetic miRNAs that were identical to the published sequences.

miRNAs and transfection

The miRCURY locked nucleic acid (LNA) modified antisense oligonucleotides to EBV BART miRNAs (anti-EBV-miR-BART) were purchased from Exiqon. The sequence of the antisense oligonucleotides are as follows: Scramble Negative Control (5′-GTGTAACACGTCTATACGCCCA -3′); anti-EBV-miR-BART9 (5′- ACTACGGGACCCATGAAGTGTTA- 3′); anti-EBV-miR-BART17-5p (5′- CTTGTATGCCTGCGTCCTCTTA-3′); anti-EBV-miR-BART7 (5′- CCCTGGACACTGGACTATGATG-3′); anti-EBV-miR-BART1-3p (5′- GACATAGTGGATAGCGGTG-CTA-3′); anti-EBV-miR-BART1-5p (5′- CACAGCACGTCAC-TTCCACTAAGA-3′); anti-EBV-miR-BART16 (5′FAM- AGAG-CACACACCCACTCTATCTAA-3′). Precursor EBV miRNA (pre-EBV-miR) was designed based on the sequence in miRBase sequence database (http://microrna.sanger.ac.uk/sequences). pre-EBV-miR-BART9 (5′- UAACACUUCAUGGGUCCCGUAGU-3′) and precursor Negative control miRNA (pre-NegCtrl) were ordered from Ambion/Applied Biosystems.

SNK6 and SNT 16 cells were seeded at 1×10^6 cells in 24- well tissue culture plates and transfected with antisense or precursor miRNAs using Oligofectamine or Lipofectamine RNAimax according to the manufacturer's protocol. Transfection efficiency of the miRNAs in SNK6 and SNT 16 cells was determined with FAM labeled EBV- BART16 miRNA and was found to be nearly 98% as determined by flow cytometry (data not shown). Cell viability following transfections was measured by Trypan Blue exclusion and found to be ~95%.

RT-real time PCR for EBV mRNAs

Independent transfections of anti-EBV-miR-BART 9 or pre-EBV-miR-BART 9 were performed in SNK6 cells. The controls transfected were either Scramble-miRNA (Exiqon) or Precursor-Negative Control (Pre-NegCtrl) (Applied Biosystems), respectively, as described above. Total RNA was isolated using RNeasy mini kit (Qiagen) and RT-real-time-PCR assays carried out for quantification of LMP1 and α-tubulin levels using the Bio-Rad MyIQ single color detection system. Briefly, 10 ng of cellular RNA was reverse transcribed into cDNA using the iScript cDNA synthesis kit (Bio-Rad) in a 20 μl reaction using the manufacturer's protocol. Quantitative real-time PCR was performed using 3 μl of the synthesized cDNA and the iQ™ SYBR Green Supermix (Bio-Rad). PCR reactions were carried out in 96-well format using a Bio-Rad iCycler. Analysis was done by the MyIQ software program (Bio-Rad) and the fold-changes were calculated using the ΔΔCt method as previously described [47] with α-Tubulin as the housekeeping gene control. The primer sequences used for LMP1 have been described previously [48] and were LMP1 (forward) - 5′

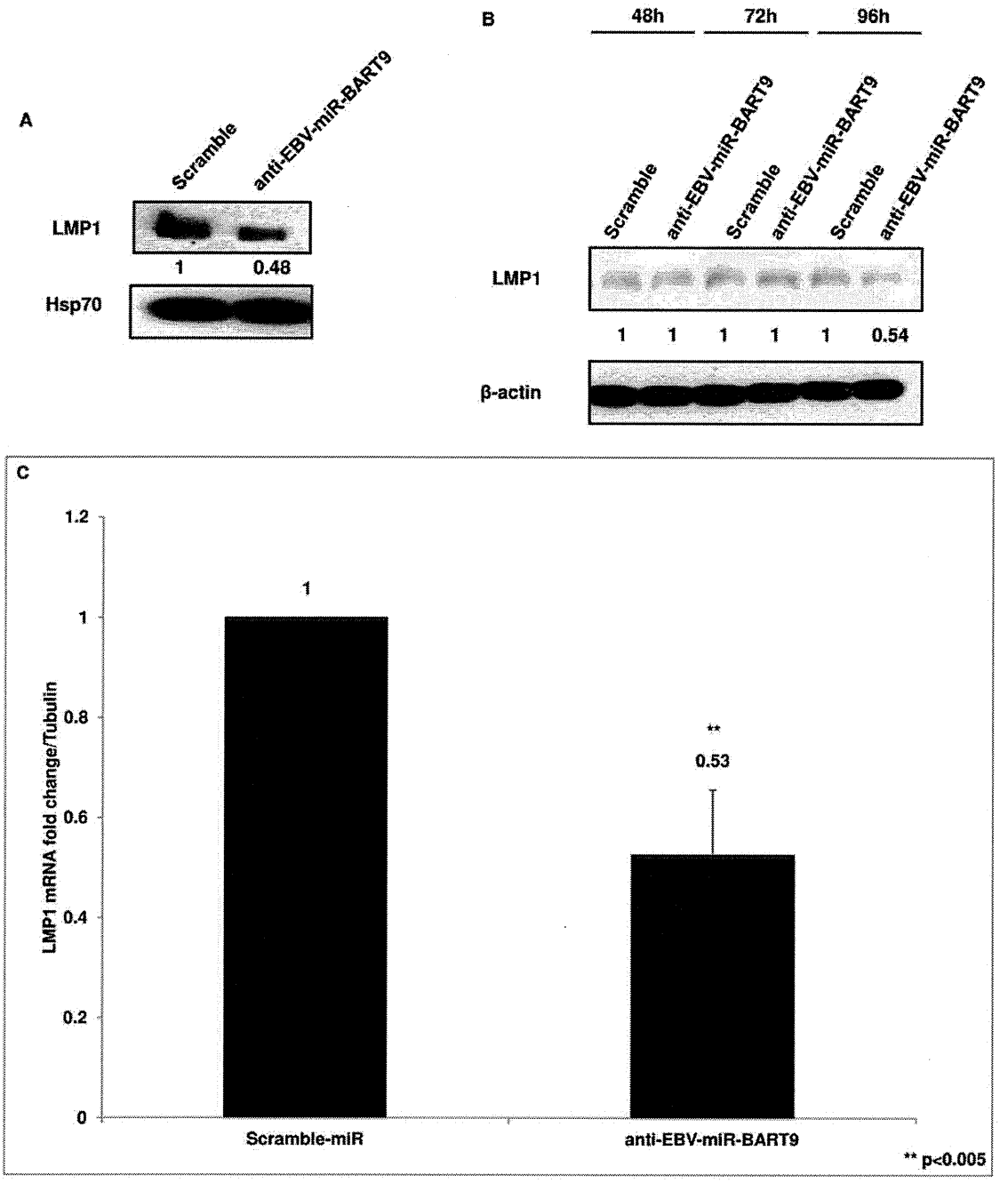

Figure 4. Immunoblot and Q-RT-PCR analysis of LMP1 expression in SNK6 following inhibition of EBV-BART9 miRNA. (**A**) SNK6 cells were transfected with anti-EBV-BART9 miRNA or Scramble control miRNA and cell lysates prepared 96 hours post-transfection. LMP1 protein expression was analyzed in immunoblots. When compared to cells transfected with control miRNA and normalized to β-actin loading control, quantification of immunoblots showed that BART9 inhibition reduced LMP1 protein levels by ~50%. (**B**) SNK6 cells were transfected with control or anti-EBV-BART9 miRNA and samples collected every 24 hours in a time-course experiment. Cell lysates were prepared and immunoblot analysis carried out to determine LMP1 expression. Quantification of LMP1 levels using Image J as described above showed that LMP1 protein levels are reduced only at later time-point. (**C**) SNK6 cells were transfected with either anti-EBV-BART9 or control miRNA and cells collected 96 hours post-transfection. Total RNA was extracted and cDNA synthesized using iScript cDNA synthesis kit. Using LMP1 specific primers, Q-PCR was carried out and data analyzed using the ΔΔCt method. Data shown is the average ± SD from three independent experiments. (** represents p value of <0.005 in a paired t-test).
doi:10.1371/journal.pone.0027271.g004

AGCCCTCCTTGTCCTCTATTCCTT 3′, LMP1 (reverse) - 5′ACCAAGTCGCCAGAGAATCTCCAA 3′. The primers for α-Tubulin were, α-Tubulin (forward) - 5′ CCTGACCACCCACACCACAC 3′, α-Tubulin (reverse) - 5′ TCTGACTGATGAGGCGGTTGAG 3′.

Cell proliferation functional assay

SNK6 and SNT16 cells were seeded in 96 well plates at 8×10^5 cells in 100 µl/well and transfected with 100 pmol of indicated anti-EBV-miRNAs or pre-EBV-miRNAs or control Scramble-miRNA or Pre-Neg-Ctrl. In some experiments, the cells were

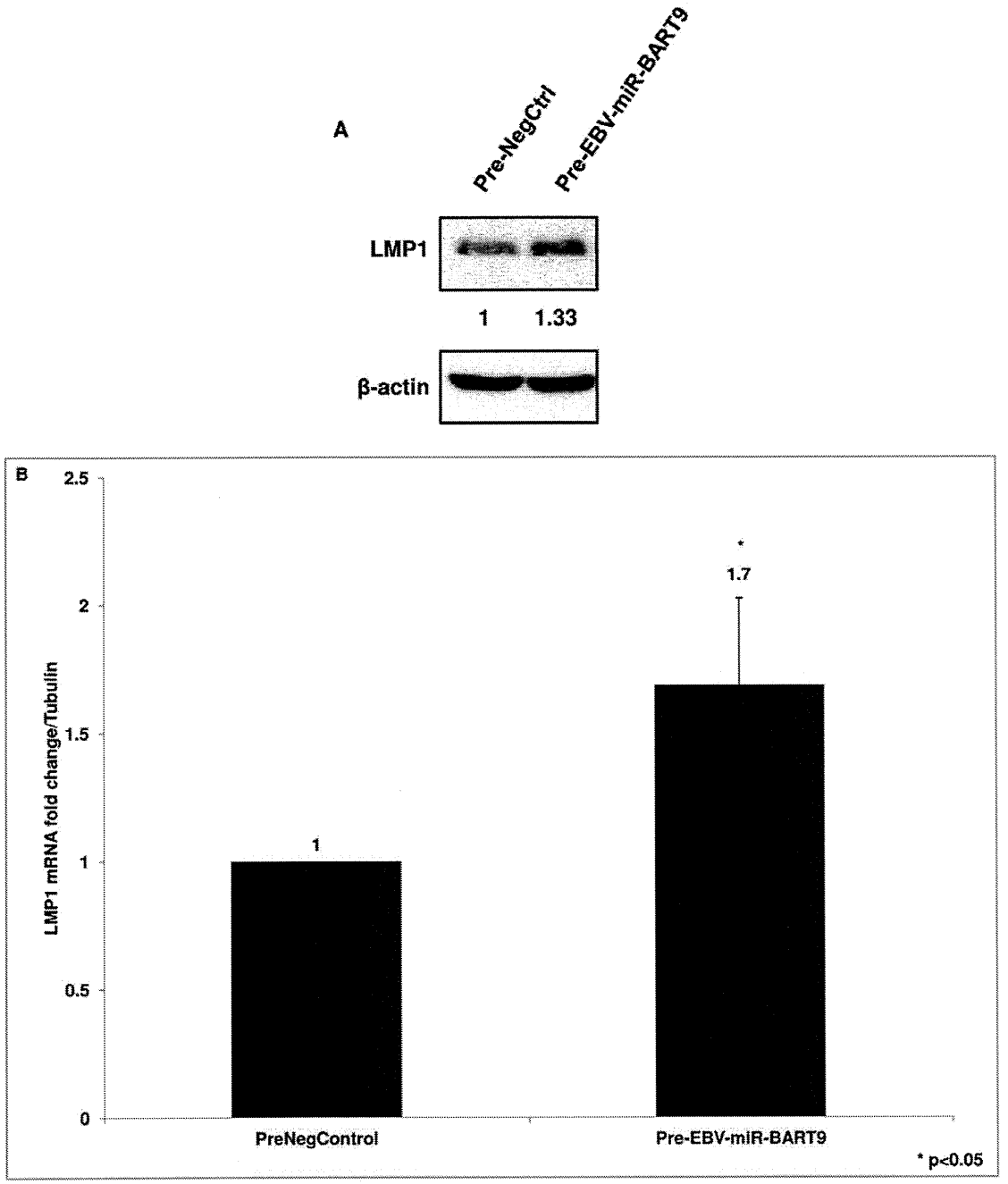

Figure 5. Precursor EBV-BART9 miRNA increases LMP1 protein and mRNA levels in SNK6 cells. (**A**) SNK6 cells were transfected with precursor EBV-BART9 or control miRNA. The cells were collected 96 hours post-transfection and cell lysates prepared for immunoblot analysis. Quantification of immunoblots showed a ~33% increase in LMP1 protein levels in cells transfected with EBV miRNA compared to control miRNA transfected cells when normalized to loading control. Data shown is a representative immunoblot from three independent experiments. (**B**) Total RNA was extracted from SNK6 cells transfected with precursor EBV-BART9 or control miRNA. Following cDNA synthesis, LMP1 mRNA levels were analyzed by Q-RT-PCR. Data presented is the average ± SD from three independent experiments. (* represents p value of <0.05 in a paired t-test).
doi:10.1371/journal.pone.0027271.g005

seeded at 1×10^6 cells/well. After overnight incubation, the cells were transferred into 24 well tissue culture plates. Cells were collected every 24 hours and analyzed for cell number and viability using the Becton-Dickinson Vi-CELL counter at the Baylor College of Medicine Flow Cytometry Core. The cell counter uses trypan blue exclusion to automatically stain and count cells, as well as assay cell size and viability.

Immunoblotting

Cells following treatment were lysed with EBCD buffer (50 mM Tris-HCl, pH 8.0, 120 mM NaCl, 0.5% NP-40, 5 mM dithiothreitol) containing protease inhibitor cocktail (Sigma). Immunoblotting was performed as described previously [49]. Monoclonal antibodies used in this study include, LMP1 (S12), EBNA-LP (JF186), EBNA3C (A10), and EBNA2 (R3). Other antibodies

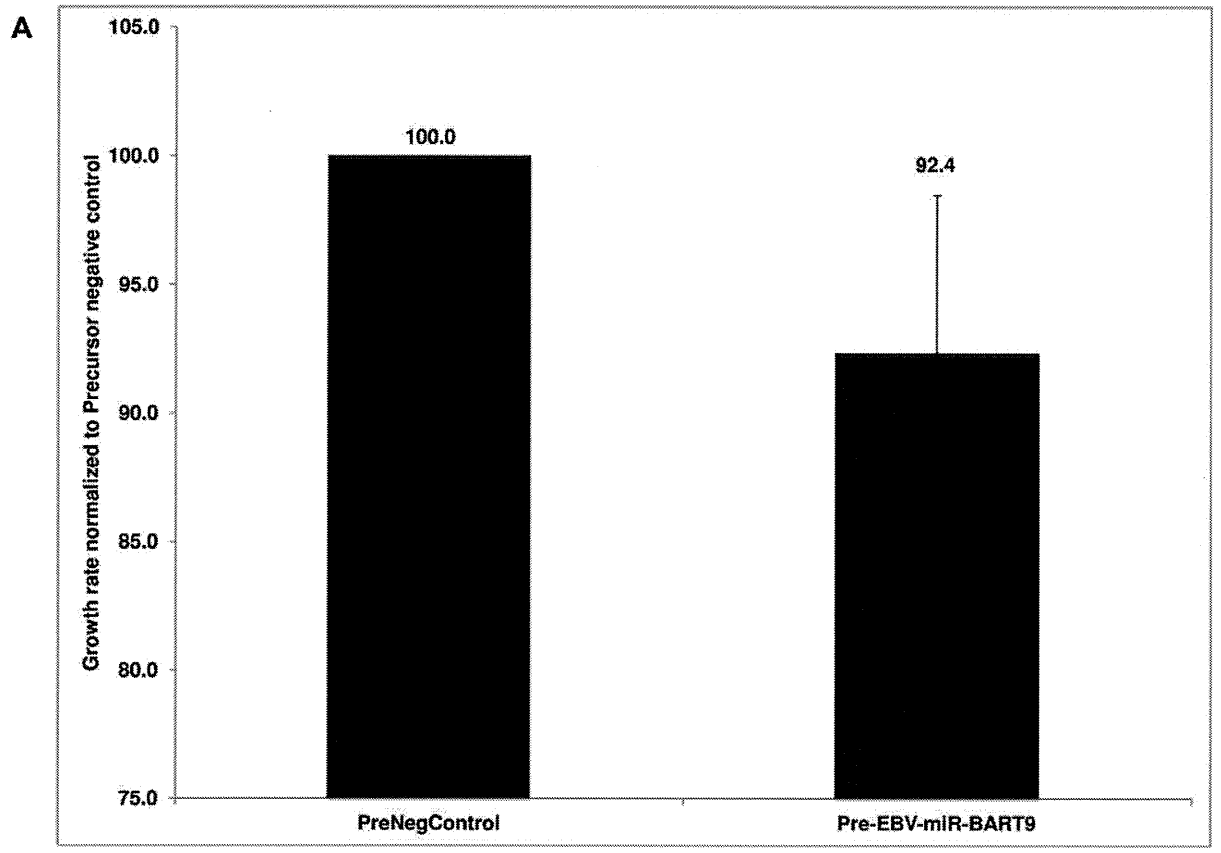
A
105.0
100.0
95.0
90.0
85.0
80.0
75.0
Growth rate normalized to Precursor negative control
100.0
92.4
PreNegControl
Pre-EBV-miR-BART9

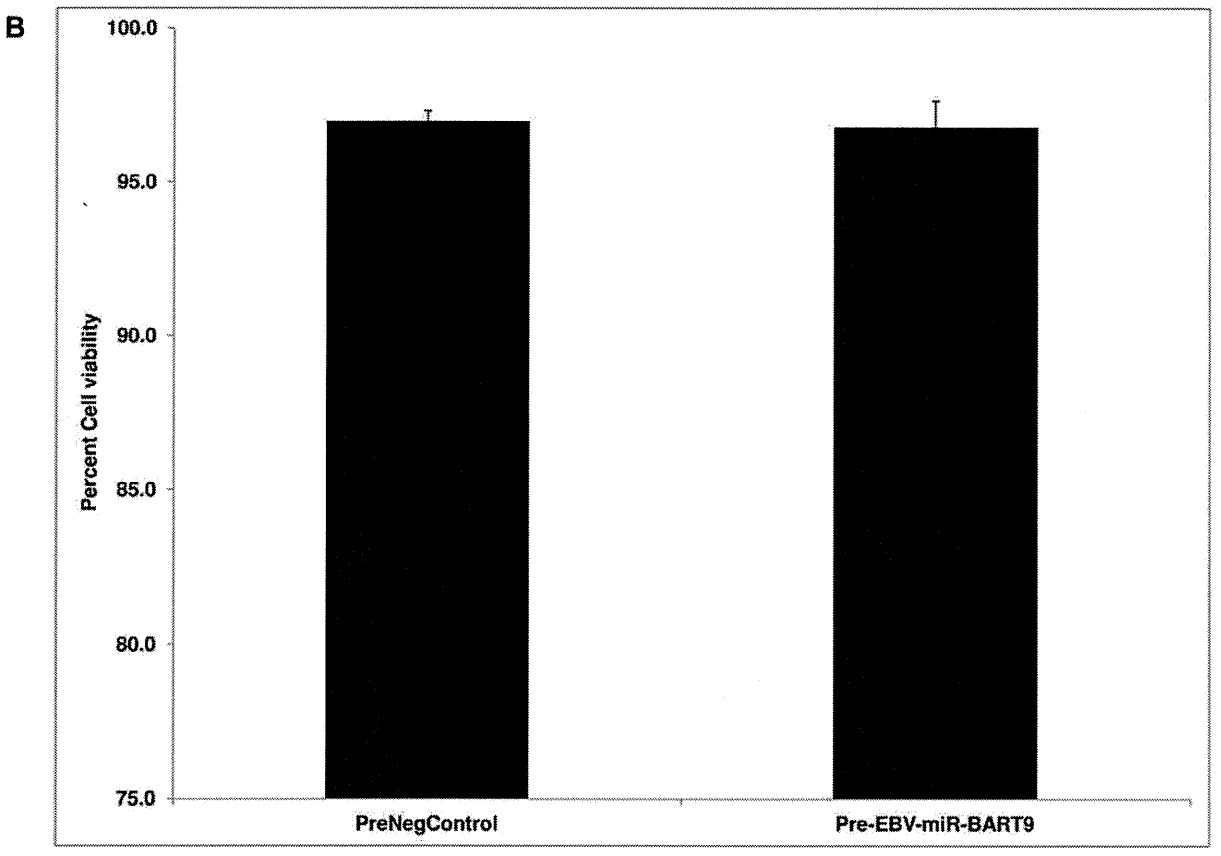
B
100.0
95.0
90.0
85.0
80.0
75.0
Percent Cell viability
PreNegControl
Pre-EBV-miR-BART9

Figure 6. Increasing EBV-BART9 miRNA level has a subtle effect on SNK6 growth rate. (**A**) Precursor EBV-BART9 miRNA or control miRNA were transfected into SNK6 cells and samples collected every 24 hours for three days. Growth rate of SNK6 cells was determined by calculating cell numbers. When normalized to cell numbers in control miRNA transfected cells, there was ~8% reduction in SNK6 growth rate. The data shown is the average ± SD from three independent experiments. (**B**) In the experiments described above, SNK6 were analyzed for viability by Trypan blue exclusion in a Vi-CELL counter at every time point. The data shown is the cell viability at 72 hours post-transfection and is the average ± SD from three independent experiments.
doi:10.1371/journal.pone.0027271.g006

obtained commercially included EBNA1 (1EB12, Santa Cruz), Zta (Argene), β-Actin (Sigma) and α-tubulin (Sigma). HRP secondary antibodies were obtained from Jackson Immunolaboratories and Western blots were developed using the SuperSignal West pico kit (Thermo Scientific). Immunoblots were quantified using Image J software [50].

Acknowledgments

We acknowledge Baylor College of Medicine Cytometry Core for flow cytometry analysis.

Author Contributions

Conceived and designed the experiments: RR APR PDL. Performed the experiments: RR HD DG JT PDL. Analyzed the data: RR HD DG JT PDL. Contributed reagents/materials/analysis tools: NS. Wrote the paper: RR APR PDL.

References

1. Shah KM, Young LS (2009) Epstein-Barr virus and carcinogenesis: beyond Burkitt's lymphoma. Clin Microbiol Infect 15: 982–988.
2. Thorley-Lawson DA (2005) EBV the prototypical human tumor virus–just how bad is it? J Allergy Clin Immunol 116: 251–261; quiz 262.
3. Cai X, Schafer A, Lu S, Bilello JP, Desrosiers RC, et al. (2006) Epstein-Barr virus microRNAs are evolutionarily conserved and differentially expressed. PLoS Pathog 2: e23.
4. Chen SJ, Chen GH, Chen YH, Liu CY, Chang KP, et al. (2010) Characterization of Epstein-Barr virus miRNAome in nasopharyngeal carcinoma by deep sequencing. PLoS One 5.
5. Grundhoff A, Sullivan CS, Ganem D (2006) A combined computational and microarray-based approach identifies novel microRNAs encoded by human gamma-herpesviruses. RNA 12: 733–750.
6. Pfeffer S, Sewer A, Lagos-Quintana M, Sheridan R, Sander C, et al. (2005) Identification of microRNAs of the herpesvirus family. Nat Methods 2: 269–276.
7. Pratt ZL, Kuzembayeva M, Sengupta S, Sugden B (2009) The microRNAs of Epstein-Barr Virus are expressed at dramatically differing levels among cell lines. Virology 386: 387–397.
8. Selbach M, Schwanhausser B, Thierfelder N, Fang Z, Khanin R, et al. (2008) Widespread changes in protein synthesis induced by microRNAs. Nature 455: 58–63.
9. Cullen BR (2009) Viral and cellular messenger RNA targets of viral microRNAs. Nature 457: 421–425.
10. Barth S, Pfuhl T, Mamiani A, Ehses C, Roemer K, et al. (2008) Epstein-Barr virus-encoded microRNA miR-BART2 down-regulates the viral DNA polymerase BALF5. Nucleic Acids Res 36: 666–675.
11. Lo AK, To KF, Lo KW, Lung RW, Hui JW, et al. (2007) Modulation of LMP1 protein expression by EBV-encoded microRNAs. Proc Natl Acad Sci U S A 104: 16164–16169.
12. Choy EY, Siu KL, Kok KH, Lung RW, Tsang CM, et al. (2008) An Epstein-Barr virus-encoded microRNA targets PUMA to promote host cell survival. J Exp Med 205: 2551–2560.
13. Xia T, O'Hara A, Araujo I, Barreto J, Carvalho E, et al. (2008) EBV microRNAs in primary lymphomas and targeting of CXCL-11 by ebv-mir-BHRF1-3. Cancer Res 68: 1436–1442.
14. Cameron JE, Fewell C, Yin Q, McBride J, Wang X, et al. (2008) Epstein-Barr virus growth/latency III program alters cellular microRNA expression. Virology 382: 257–266.
15. Cameron JE, Yin Q, Fewell C, Lacey M, McBride J, et al. (2008) Epstein-Barr virus latent membrane protein 1 induces cellular MicroRNA miR-146a, a modulator of lymphocyte signaling pathways. J Virol 82: 1946–1958.
16. Lu F, Weidmer A, Liu CG, Volinia S, Croce CM, et al. (2008) Epstein-Barr virus-induced miR-155 attenuates NF-kappaB signaling and stabilizes latent virus persistence. J Virol 82: 10436–10443.
17. Yin Q, McBride J, Fewell C, Lacey M, Wang X, et al. (2008) MicroRNA-155 is an Epstein-Barr virus-induced gene that modulates Epstein-Barr virus-regulated gene expression pathways. J Virol 82: 5295–5306.
18. Amoroso R, Fitzsimmons L, Thomas WA, Kelly GL, Rowe M, et al. (2011) Quantitative studies of Epstein-Barr virus-encoded microRNAs provide novel insights into their regulation. J Virol 85: 996–1010.
19. Cosmopoulos K, Pegtel M, Hawkins J, Moffett H, Novina C, et al. (2009) Comprehensive profiling of Epstein-Barr virus microRNAs in nasopharyngeal carcinoma. J Virol 83: 2357–2367.
20. Imig J, Motsch N, Zhu JY, Barth S, Okoniewski M, et al. (2011) microRNA profiling in Epstein-Barr virus-associated B-cell lymphoma. Nucleic Acids Res 39: 1880–1893.
21. Kim do N, Chae HS, Oh ST, Kang JH, Park CH, et al. (2007) Expression of viral microRNAs in Epstein-Barr virus-associated gastric carcinoma. J Virol 81: 1033–1036.
22. Nagata H, Konno A, Kimura N, Zhang Y, Kimura M, et al. (2001) Characterization of novel natural killer (NK)-cell and gammadelta T-cell lines established from primary lesions of nasal T/NK-cell lymphomas associated with the Epstein-Barr virus. Blood 97: 708–713.
23. Zhang Y, Nagata H, Ikeuchi T, Mukai H, Oyoshi MK, et al. (2003) Common cytological and cytogenetic features of Epstein-Barr virus (EBV)-positive natural killer (NK) cells and cell lines derived from patients with nasal T/NK-cell lymphomas, chronic active EBV infection and hydroa vacciniforme-like eruptions. Br J Haematol 121: 805–814.
24. Aozasa K, Takakuwa T, Hongyo T, Yang WI (2008) Nasal NK/T-cell lymphoma: epidemiology and pathogenesis. Int J Hematol 87: 110–117.
25. Kohrt H, Advani R (2009) Extranodal natural killer/T-cell lymphoma: current concepts in biology and treatment. Leuk Lymphoma 50: 1773–1784.
26. Tao Q, Young LS, Woodman CB, Murray PG (2006) Epstein-Barr virus (EBV) and its associated human cancers–genetics, epigenetics, pathobiology and novel therapeutics. Front Biosci 11: 2672–2713.
27. Harabuchi Y, Yamanaka N, Kataura A, Imai S, Kinoshita T, et al. (1990) Epstein-Barr virus in nasal T-cell lymphomas in patients with lethal midline granuloma. Lancet 335: 128–130.
28. Ho FC, Srivastava G, Loke SL, Fu KH, Leung BP, et al. (1990) Presence of Epstein-Barr virus DNA in nasal lymphomas of B and 'T' cell type. Hematol Oncol 8: 271–281.
29. Kanavaros P, Lescs MC, Briere J, Divine M, Galateau F, et al. (1993) Nasal T-cell lymphoma: a clinicopathologic entity associated with peculiar phenotype and with Epstein-Barr virus. Blood 81: 2688–2695.
30. Garzon R, Croce CM (2008) MicroRNAs in normal and malignant hematopoiesis. Curr Opin Hematol 15: 352–358.
31. Bueno MJ, Perez de Castro I, Malumbres M (2008) Control of cell proliferation pathways by microRNAs. Cell Cycle 7: 3143–3148.
32. Young LS, Rickinson AB (2004) Epstein-Barr virus: 40 years on. Nat Rev Cancer 4: 757–768.
33. Eliopoulos AG, Dawson CW, Mosialos G, Floettmann JE, Rowe M, et al. (1996) CD40-induced growth inhibition in epithelial cells is mimicked by Epstein-Barr Virus-encoded LMP1: involvement of TRAF3 as a common mediator. Oncogene 13: 2243–2254.
34. Yamanaka Y, Tagawa H, Takahashi N, Watanabe A, Guo YM, et al. (2009) Aberrant overexpression of microRNAs activate AKT signaling via down-regulation of tumor suppressors in natural killer-cell lymphoma/leukemia. Blood 114: 3265–3275.
35. Calin GA, Croce CM (2006) MicroRNA signatures in human cancers. Nat Rev Cancer 6: 857–866.
36. Chiang AK, Tao Q, Srivastava G, Ho FC (1996) Nasal NK- and T-cell lymphomas share the same type of Epstein-Barr virus latency as nasopharyngeal carcinoma and Hodgkin's disease. Int J Cancer 68: 285–290.
37. Esquela-Kerscher A, Slack FJ (2006) Oncomirs - microRNAs with a role in cancer. Nat Rev Cancer 6: 259–269.
38. Ivanovska I, Ball AS, Diaz RL, Magnus JF, Kibukawa M, et al. (2008) MicroRNAs in the miR-106b family regulate p21/CDKN1A and promote cell cycle progression. Mol Cell Biol 28: 2167–2174.
39. Galardi S, Mercatelli N, Giorda E, Massalini S, Frajese GV, et al. (2007) miR-221 and miR-222 expression affects the proliferation potential of human prostate carcinoma cell lines by targeting p27Kip1. J Biol Chem 282: 23716–23724.
40. Sample J, Kieff E (1990) Transcription of the Epstein-Barr virus genome during latency in growth-transformed lymphocytes. J Virol 64: 1667–1674.

41. Kaykas A, Sugden B (2000) The amino-terminus and membrane-spanning domains of LMP-1 inhibit cell proliferation. Oncogene 19: 1400–1410.
42. Narbonnet S, Mariame B (2006) The Epstein-Barr virus oncoprotein LMP1 inhibits the activity of viral or cellular promoters without inducing cytostasis. Virology 350: 381–393.
43. Brooks JM, Lee SP, Leese AM, Thomas WA, Rowe M, et al. (2009) Cyclical expression of EBV latent membrane protein 1 in EBV-transformed B cells underpins heterogeneity of epitope presentation and CD8+ T cell recognition. J Immunol 182: 1919–1928.
44. Johansson P, Jansson A, Ruetschi U, Rymo L (2010) The p38 signaling pathway upregulates expression of the Epstein-Barr virus LMP1 oncogene. J Virol 84: 2787–2797.
45. Bolstad BM, Irizarry RA, Astrand M, Speed TP (2003) A comparison of normalization methods for high density oligonucleotide array data based on variance and bias. Bioinformatics 19: 185–193.
46. Chen C, Ridzon DA, Broomer AJ, Zhou Z, Lee DH, et al. (2005) Real-time quantification of microRNAs by stem-loop RT-PCR. Nucleic Acids Res 33: e179.
47. Haaland RE, Yu W, Rice AP (2005) Identification of LKLF-regulated genes in quiescent CD4+ T lymphocytes. Mol Immunol 42: 627–641.
48. Goormachtigh G, Ouk TS, Mougel A, Tranchand-Bunel D, Masy E, et al. (2006) Autoactivation of the Epstein-Barr virus oncogenic protein LMP1 during type II latency through opposite roles of the NF-kappaB and JNK signaling pathways. J Virol 80: 7382–7393.
49. Ramakrishnan R, Dow EC, Rice AP (2009) Characterization of Cdk9 T-loop phosphorylation in resting and activated CD4(+) T lymphocytes. J Leukoc Biol 86: 1345–1350.
50. Abramoff MD, Magelhaes PJ, Ram SJ (2004) Image Processing with ImageJ. Biophotonics International 11: 36–42.

NOTE *Bacteriology*

Mycoplasma ovis Detected in Free-Living Japanese Serows, *Capricornis crispus*

Yoshihiro OHTAKE[1], Ikuo NISHIZAWA[1], Makoto SATO[1], Yusaku WATANABE[1], Takashi NISHIMURA[2], Kazuei MATSUBARA[2], Kazuya NAGAI[3] and Ryô HARASAWA[1]*

[1]*Departments of Veterinary Microbiology,* [2]*Animal Science and* [3]*Cryobiofrontier Research Center, Faculty of Agriculture, Iwate University, Morioka 020–8550, Japan*

(Received 5 September 2010/Accepted 2 October 2010/Published online in J-STAGE 15 October 2010)

ABSTRACT. Nineteen blood samples collected from free-ranging wild Japanese serows, *Capricornis crispus*, between 2006 and 2008 in Iwate prefecture were examined for the hemoplasma infection by real-time PCR targeting the 16S rRNA gene. Five (26.3%) out of the 19 samples were positive in real-time PCR with an average melting temperature at 85.18°C. The positive samples in the real-time PCR were reconfirmed by conventional PCR, and one of them was successful for direct DNA sequencing. The nucleotide sequence of the 16S rRNA gene of the representative stain was identical to that of *Mycoplasma ovis*. This was the first demonstration of hemotropic mycoplasma infections among the free-living Japanese serows in Japan.

KEY WORDS: hemoplasma, Japanese serow.

J. Vet. Med. Sci. 73(3): 371–373, 2011

Hemoplasmas are epierythrocytic mycoplasmas, but have never been cultured *in vitro* [8]. Hemoplasmas infections have been reported in wild ungulates such as reindeer (*Rangifer tarandus*) raised on a farm in Michigan [14] and splenectomized deer captured from a wild population in Texas [7] in the United States. However prevalence of hemoplasma infections in free-living ungulates has not well been understood. Recently, we have newly detected hemoplasma infections in wild sika deer in Iwate Prefecture [17]. In the present study, we subsequently examined for hemoplasma infections in free-living Japanese serows (*Capricornis crispus*).

Whole blood samples collected from 19 free-living Japanese serows during three years from 2006 to 2008 in the Iwate prefecture were examined for the presence of hemoplasmas by the real-time PCR procedure using the hemoplasma specific primers to amplify the 16S rRNA gene region. Heparinized-blood or clots of blood samples were stored at –20°C prior to analysis. Smear preparations ware not available because of frozen blood samples. Total DNA was extracted from 200 μl of the whole blood samples by using the QIAamp DNA Blood Mini Kit (QIAGEN, Hilden, Germany) according to the manufacturer's instructions, eluting into 200 μl of buffer AE, and stored at –20°C until examination in the PCR assays.

Real-time PCR was performed in a SmartCycler instrument (Cepheid, Sunnyvale, Calif., U.S.A.) with SYBR Premix Ex *Taq* (Code #RR041A, TaKaRa Bio., Shiga). Hemoplasma specific PCR primers (forward primer: 5'-ATATTCCTACGGGAAGCAGC-3' and reverse primer: 5'-ACCGCAGCTGCTGGCACATA-3') for the 16S rRNA gene of hemoplasmas were used as described previously [12]. After real-time PCR, melting experiment was performed from 60 to 95°C at 0.2°C/sec with smooth curve setting averaging one point, by using a nonspecific fluorescent dye, SYBR Green I. Melting peaks were visualized by plotting the first derivative against the melting temperature (*Tm*) as described previously [3]. By Preliminary screening by real-time PCR detected five (26.3%) out of the 19 samples were positive for hemoplasma infections, and an average *Tm* was 85.18°C (Fig. 1). High-resolution of melting curve experiments allow discrimination of variations in nucleotide sequences, which indicate specificity of the real-time PCR [11].

The positive samples were re-examined by conventional PCR targeting the 16S rRNA gene for nucleotide sequencing. The conventional PCR was carried out with 50-μl reaction mixtures containing 1 μl of DNA solution, 0.5 μl of TaKaRa LA *Taq* ™ (5 units/μl), 5 μl of 10X LA PCR™ Buffer, 8 μl of 25 mM $MgCl_2$ (final 4.0 mM), 8 μl of dNTP mixture (2.5 mM each), 0.2 μl of forward primer (5'-ATATTCCTACGGGAAGCAGC-3', equivalent to nucleotide numbers 328 to 347 of *M. wenyonii*), reverse primer (5'-TACCTTGTTACGACTTAACT-3', equivalent to

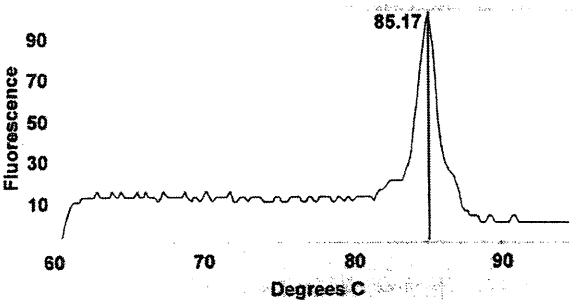

Fig. 1. Melting curve analysis of the PCR product depicted by using SYBR Green I. A representative *Tm* curve for Kamosika3 strain detected from a Japanese serows, showing a characteristic peak at 85.17°C in the melting experiments.

* CORRESPONDENCE TO: Prof. HARASAWA, R., Department of Veterinary Microbiology, Faculty of Agriculture, Iwate University, Morioka 020–8550, Japan.
e-mail: harasawa-tky@umin.ac.jp

nucleotide numbers 1446 to 1465 of *M. wenyonii*) (50 pmol/μl each) and water to a final volume of 50 μl. After the mixture was overlaid with 20 μl of mineral oil, the reaction cycle was carried out 35 times with denaturation at 94°C for 30 sec, annealing at 60°C for 120 sec and extension at 72°C for 60 sec in a thermal cycler.

The PCR products were fractionated on horizontal, submerged 1.0% SeaKem GTG agarose gels (FMC Bioproducts, Rockland, Me., U.S.A.) in TAE (40 mM Tris, pH8.0, 5 mM sodium acetate, 1 mM disodium ethylenediaminetetracetate) buffer at 50 volts for 60 min. After electrophoresis, the gels were stained in ethidium bromide solution (0.4 μg/ml) for 15 min. DNA was extracted by using NucleoSpin Extract II kit (Macherey-Nagel, Düren, Germany) and was subjected to direct sequencing in a 3500 Genetic Analyzer (Applied Biosystems, Foster City, Calif., U.S.A.). Only one sample developed a clear nucleotide sequence. This suggests that the other samples were of mixed-infection. The nucleotide sequence of the partial 16S rRNA gene has been deposited in the DDBJ, EMBL, GSDB and NCBI nucleotide sequence databases under the accession number AB571119.

In the present study, nucleotide sequences of the 16S rRNA gene from the Kamosika3 strain along with the 13 established hemoplasma species were aligned using CLUSTAL W (version 1.83; DDBJ) with further adjustment made manually by eyes as necessary [16]. An unrooted phylogenetic tree constructed by the algorithms implemented in the PHYLIP program (DDBJ) using the neighbor-

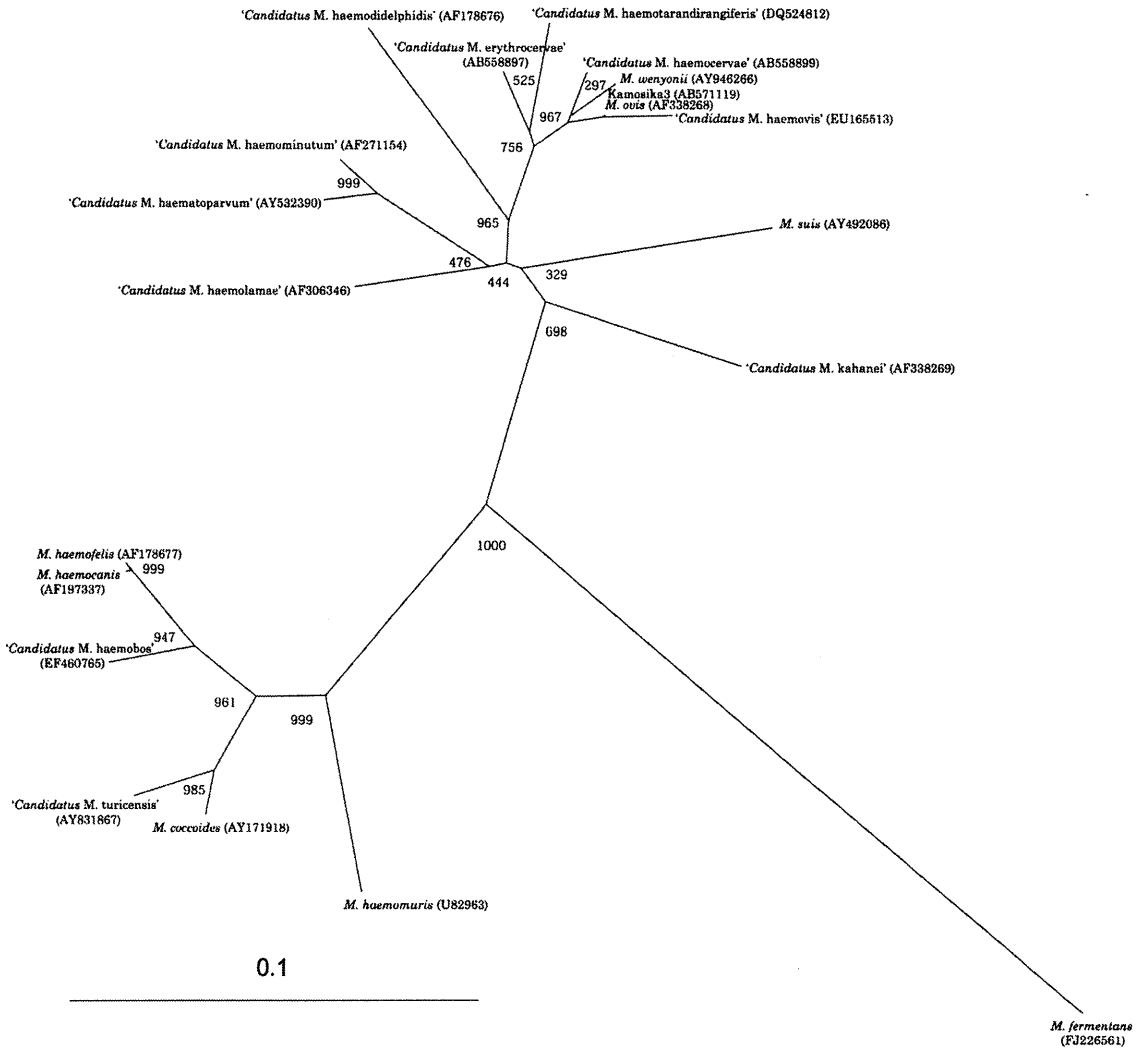

Fig. 2. Unrooted phylogenetic tree based on the 16S rRNA gene sequence comparison among mycoplasmas including 18 hemoplasma species (accession numbers are given in a parenthesis) and a Kamosika3 strain. Genetic distances were computed with CLUSTAL W [16]. A nucleotide sequence of the 16S rRNA gene of *M. fermentans* PG18 strain with accession number FJ226561 was included as an out-group. Numbers in the relevant branches refer to the values of boot-strap probability of 1,000 replications. Scale bar indicates the estimated evolutionary distance.

joining method [13] indicated that the hemoplasma strain detected in the Japanese serows was most closely related to *Mycoplasma ovis* (Fig. 2) which was also close to '*Candidatus* M. haemovis' [4]. Similarity of the 16S rRNA gene sequences between Kamosika3 strain and *M. ovis* ranged from 99.5 to 99.8%, while 96.3 to 96.6% between Kamosika3 and '*Candidatus* M. haemovis'.

The Japanese serows, one of Japan's official national treasures, usually live on steep, thickly wooded hillsides on the islands of Honshu, Kyushu and Shikoku in Japan. All the Japanese serows examined were found in Morioka and Rikuzentakata or their vicinal areas. They have been problematic for taxonomists due to their unique characteristics. Although the serows were tentatively given the generic name *Nemorhaedus* [2], recent study indicates that the Japanese serows are distinct from gorals, the genus *Nemorhaedus*, and should be allocated to the genus *Capricornis* [9]. The serows and sheep (*Ovis aries*) are both the members in the subfamily *Caprinae* of the family *Bovidae*.

Mycoplasma ovis is prevailed world-widely and causative of hemolytic anemia in sheep and goats of all ages from 4 weeks upwards [1, 10], resulting in economic losses. Young sheep, particularly weaners, are most severely affected but older sheep can also be noticeably affected. The effect of *M. ovis* infection is more severe if sheep are stressed by other conditions such as internal parasites or malnutrition. Deaths may occur in severely affected young sheep, if they are stressed by yarding. Role of *M. ovis* in wild ungulates is largely unknown, though there is some evidence that variants of this particular hemoplasma species have also been isolated from humans [5, 15], suggesting a zoonotic pathogen. We first demonstrated *M. ovis* infections in free-living Japanese serows. Therefore, it will be necessary to further examine that the wildlife could serve as a reservoir for hemoplasma infections in not only domestic animals, but also humans, though there has never been reported on *M. ovis* infections in sheep or goats in this country.

REFERENCES

1. Aguirre, D.H., Thompson, C., Neumann, R.D., Salatin, A.O., Gaido, A.B. and Torioni de Echaide, S. 2009. Brote de micplasmosis clinica por *Mycoplasma ovis* en ovinos deSalta, Argentina. Diagnostico clinico, microbiologico y molecular. *Rev. Argentina Microbiol.* **41**: 212–214.
2. Groves, C.P. and Grubb, P. 1985. Reclassification of the serows and gorals (*Nemorhaedus Bovidae*), pp. 45–50. *In:* The Biology and Management of Mountain Ungulates (Lovari, S. ed.), Croom Helm, London.
3. Harasawa, R., Mizusawa, H., Fujii, M., Yamamoto, J., Mukai, H., Uemori, T., Asada, K. and Kato, I. 2005. Rapid detection and differentiation of the major mycoplasma contaminants in cell cultures using real-time PCR with SYBR Green I and melting curve analysis. *Microbiol. Immunol.* **49**: 859–863.
4. Hornok, S., Meli, M.L., Erdos, A., Hajtos, I., Lutz, H. and Hofmann-Lehmann, R. 2009. Molecular characterization of two different strains of haemotropic mycoplasmas from sheep flock with fatal haemolytic anaemia and concomitant *Anaplasma ovis* infection. *Vet. Microbiol.* **136**: 372–377.
5. Hu, Z., Yin, J., Shen, K., Kang, W. and Chen, Q. 2009. Outbreaks of hemotrophic mycoplasma infections in China. *Emerging Infect. Dis.* **15**: 1139–1140.
6. Kimura, M. 1980. A simple method for estimating evolutionary rates of base substitutions through comparative studies of nucleotide sequences. *J. Mol. Evol.* **16**: 111–120.
7. Kuttler, K.L., Robinson, R.M. and Rogers, W.P. 1967. Exacerbation of latent erythrocytic infections in deer following splenectomy. *Can. J. Comp. Med. Vet. Sci.* **31**: 317–319.
8. Messick, J.B. 2004. Hemotrophic mycoplasmas (hemoplasmas): a review and new insights into pathogenic potential. *Vet. Clin. Pathol.* **33**: 2–13.
9. Min, M.-S., Okamura, H., Jo, D.-J., An, J.-H., Kim, K.-S., Kim, C.-B., Shin, N.-S., Lee, M.-H., Han, C.-H., Voloshina, I.V. and Lee, H. 2004. Molecular phylogenetic status of the Korean goral and Japanese serow based on partial sequences of the mitochondrial cytochrome b gene. *Mol. Cells* **17**: 365–372.
10. Neimark, H., Hoff, B., and Ganter, M. 2004. *Mycoplasma ovis* comb. nov. (formerly *Eperythrozoon ovis*), an epierythrocytic agent of haemolytic anaemia is sheep and goats. *Int. J. Syst. Evol. Microbiol.* **54**: 365–371.
11. Nellaker, C., Uhrzander, F., Tyrcha, J. and Karlsson, H. 2008. Mixture models for analysis of melting tenperature data. *BMC Bioinformatics* **9**: 370. doi:10.1186/1471–2105–9–370.
12. Nishizawa, I., Sato, M., Fujihara, M., Sato, S. and Harasawa, R. 2010. Differential detection of hemotropic *Mycoplasma* species in cattle by melting curve analysis of PCR products. *J. Vet. Med. Sci.* **72**: 77–79. (Erratum, *J. Vet. Med. Sci.* **72**: E2.)
13. Saitou, N. and Nei, M. 1987. The neighbor-joining method: a new method for reconstructing phylogenetic trees. *Mol. Biol. Evol.* **4**: 406–425.
14. Stoffregen, W.C., Alt, D.P., Palmer, M.V., Olsen, S.C., Water, W.R. and Stasko, J.A. 2006. Identifiaction of a haemomycoplasma species in anemic reindeer (*Rangifer tarandus*) *J. Wildlife Dis.* **42**: 249–258.
15. Sykes, J.E., Lindsay, L.L., Maggi, R.G. and Breitschwerdt, E.B. 2010. Human co-infection with *Bartonella henselae* and two hemotropic mycoplasma variants resembling *Mycoplasma ovis*. *J. Clin. Microbiol.* **48**: 3782–3785.
16. Thompson, J.D., Higgins, D.G. and Gibson, T.J. 1994. CLUSTAL W: improving the sensitivity of progressive multiple sequence alignment through sequence weighting, position-specific gap penalties and weight matrix choice. *Nucleic Acids Res.* **22**: 4673–4680.
17. Watanabe, Y., Fujihara, M., Obara, H., Matsubara, K., Yamauchi, K. and Harasawa, R. 2010. Novel hemoplasma species detected in free-ranging sika deer (*Cervus nippon*). *J. Vet. Med. Sci.* **72**: 1527–1530.

NOTE *Bacteriology*

A Feline Hemoplasma, '*Candidatus* Mycoplasma haemominutum', Detected in Dog in Japan

Hisato OBARA[1,2,3], Masatoshi FUJIHARA[1,3], Yusaku WATANABE[1,3], Hisaya K. ONO[3] and Ryô HARASAWA[1,3]*

[1]*Department of Veterinary Microbiology, School of Veterinary Medicine, Faculty of Agriculture, Iwate University, Morioka 020–8550,* [2]*Will Animal Hospital, Sendai, Miyagi 983–0826 and* [3]*Department of Applied Veterinary Science, The United Graduate School of Veterinary Sciences, Gifu University, Gifu 501–1193, Japan*

(Received 22 November 2010/Accepted 14 January 2011/Published online in J-STAGE 28 January 2011)

ABSTRACT. We examined for '*Candidatus* Mycoplasma haemominutum' infection in 167 blood samples collected from domestic dogs between 2008 and 2009 in the Tohoku area, Japan, and found 5 (3.0%) were positive by PCR assay. This is the first demonstration of '*Candidatus* Mycoplasma haemominutum', a feline haemotropic mycoplasma, in the dogs raised in Japan.

KEY WORDS: 16S rRNA, canine, feline hemoplasma, mycoplasma.

J. Vet. Med. Sci. 73(6): 841–843, 2011

Hemoplasmas, hematropic mycoplasmas, infect the erythrocytes and are causative of hemolytic anemia and thrombocytosis in animal [16]. Currently, three hemoplasma species, *Mycoplasma haemofelis*, '*Candidatus* Mycoplasma haemominutum', and '*Candidatus* M. turicensis', and tentatively "*Candidatus* M. haematoparvum-like" strain are recognized in cats [4, 5, 19, 23]. On the other hand, there are two hemoplasma species in dogs, *M. haemocanis* [15], and '*Candidatus* M. haematoparvum' [18]. In general, the *Mycoplasma* species has the strict host specificity, so there have been only a few reports of the infections in an animal species not perceived as primary host.

The inability to culture the hemoplasma *in vitro* has hampered the possibilities of investigating the epidemiology and pathogenesis of this particular microbial agent [7]. Definitive diagnosis of hemoplasma infection has mainly been depend on microscopic examination of a thin Wright-Giemsa-stained blood smear, but this method and has low sensitivity and specificity because the organisms resemble Howell-Jolly bodies or back ground debris [2], and it is more difficult to distinguish between hemoplasma species. Thus the PCR is widely used to detect hemoplasmas because of its sensitivity [1, 21].

Haemoplasmosis caused by *M. haemofelis* can lead to life-threatening hemolytic anemia in cats, whereas clinical signs in haemoplasmosis caused by '*Candidatus* M. haemominutum' and '*Candidatus* M. turicensis' have been reported to be minor or absent [5]. Dogs are latently infected with hemoplasmas, and the presence of underlying disorders such as immunosuppressive, co-infection, splenectomy, overt disease, trigger the anemia by hemoplasmas [8, 14, 22].

Although there are a few epidemiological reports on '*Candidatus* M. haemominutum' infections in dogs in only China [25] and France [12], there have been no examination on this particular hemoplasma species in Japan. Therefore, we examined for the presence of the feline hemoplasma '*Candidatus* M. haemominutum' infection in the dogs in Japan.

Ethylene diamine-tetraacetic acid (EDTA)-anticoagulated blood samples were collected from 167 pet dogs (*Canis lupus familiaris*) in the Miyagi Prefecture, Japan between 2008 and 2009. The whole blood samples were taken for clinical diagnostic and health check purposes, and the remainder was subjected to detection of '*Candidatus* M. haemominutum'. These dogs have no travel history and not been splenectomized. Date on age and sex and clinical information obtained for the dogs was incomplete. The contact history to the cats is unknown. Blood samples were stored at –80°C prior to analysis.

DNA was extracted from 200 μl anticoagulated whole blood in EDTA collected using QIAamp DNA Blood Mini Kit (QIAGEN, Hilden, Germany) according to the manufacture's instructions. DNA was eluted in 200 μl elution buffer and stored at –20°C until examination in the PCR assay.

The 16S rRNA gene of '*Candidatus* M. haemominutum' was amplified by using the following primers. A 654-bp fragment of the 16 rRNA gene was amplified using primers F1 (5'-GATTAATGCTGGTGGTATGC-3') and R1 (5'-CATTGAATTCCAGTATCTCC-3') [6]. A 403-bp fragment of the 16 rRNA gene was amplified using primers F2 (5'-TACTCTCTTAGTGGCGAACG-3') and R2 (5'-AATCAAGGCTTAATCATTTC-3') [6]. PCR was performed in two steps as followed; the first with pairs of the outer primers (F1 and R1) and the second with the inner primers (F2 and R2). The mixture for each reaction contained 5 μl of extracted DNA samples and 45 μl of the PCR master mix, which consisted of 5 μl of 10X PCR buffer, 8 μl of 2.5 mM deoxynucleoside triphosphates, 10 pmol specific outer primers, 2 units of *Tth* DNA polymerase (TOYOBO, Tokyo, Japan) and one drop of mineral oil. PCR was per-

* CORRESPONDENCE TO: HARASAWA, R., Department of Veterinary Microbiology, School of Veterinary Medicine, Faculty of Agriculture, Iwate University, Morioka 020–8550, Japan.
e-mail: harasawa-tky@umin.ac.jp

formed with an initial denaturation of 94°C for 30 sec, followed by 30 cycles of heating at 94°C for 30 sec, at 55°C for 2 min, and at 72°C for 1 min. Then 1 μl of the first PCR products were transferred into a second tube containing 49 μl of the reaction buffer as described in the first round reaction, for the second round of the same 30 cycles of amplification, but with the pair of inner primers. The PCR products were detected by electrophoresis on a 1.0% agarose gel in Tris-acetate-EDTA buffer and stained with ethidium bromide (0.4 $\mu g/ml$) and visualized under UV transilluminator, BioDoc-I Imaging System (UVP, Upland, CA, U.S.A.). Positive samples were directly subjected to DNA sequencing for identification of hemoplasma species. The nucleotide sequence of the partial 16S rRNA gene has been deposited in the DDBJ, EMBL, GSDB and NCBI nucleotide sequence databases under the accession number AB550430.

A PCR product was amplified from the five dogs, with expected band size on a 1.0 % agarose gel (Fig. 1). Three are adult dogs suffering from multi-centric lymphoma, starvation, atopic dermatitis, respectively. The other two dogs are puppy (about three months old) and have no sign of disease. No PCR products were amplified from the other 162 dogs, which did not develop any clinical sign of haemolytic anemia due to '*Candidatus* M. haemominutum' infection. Comparison of the obtained sequence (a dog suffered from lymphoma) with those corresponding sequences available in the GenBank database revealed the 98% homology to the 16S rRNA gene of '*Candidatus* M. haemominutum' (Fig. 2). We can not gain sequence of the other 4 PCR products because of insufficient PCR product in the first step PCR.

In this study, we first demonstrated that feline hemoplasma '*Candidatus* M. haemominutum' infected dogs in the northern part of Japan. The relatively low prevalence in dogs in this study, as compared to the feline infection rate of '*Candidatus* M. haemominutum' in Japan [6], may be based on the present study included healthy dog population. The study has certain limitations because of the relatively small number of case analyzed.

These dogs infected with hemoplasma had been kept in the ectoparasite-free conditions and no clinical signs of hemolytic anemia by '*Candidatus* M. haemominutum'. It is known that '*Candidatus* M. haemominutum' infection rarely results in significant clinical signs and anemia is not usually apparent in cat [5]. Similarly, dogs infected with '*Candidatus* M. haemominutum' lacked any clinical signs of hemolytic anemia. The pathogenicity of '*Candidatus* M. haemominutum' may be not severe in the dogs.

The transmission route of '*Candidatus* M. haemominutum' from the cats to the dog is currently unknown. Blood-sucking arthropods (e.g., flees, ticks) have been suspected as natural means of hemoplasma transmission [24]. However, there were not so much tick infestions due to the cold climate in the Tohoku area compared to the southern parts in Japan. It is also possible that the infection was occurred by horizontal transmission from infected cats. There is some

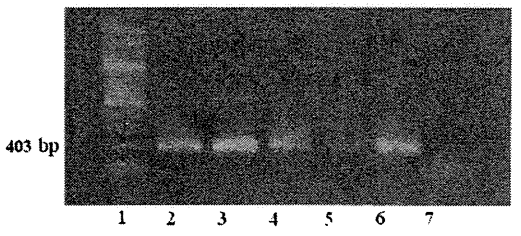

Fig. 1. A representative PCR result on detection for feline '*Candidatus* M. haemominutum' in the dogs. Lane 1 shows 200-bp DNA Ladder (TaKaRa-Bio, Shiga, Japan); Lanes 2–6 show 403-bp DNA fragment. Lanes 2, 3 and 4 dogs suffered from multi-centric lymphoma, starvation, atopic dermatitis, respectively. Lanes 5 and 6; healthy puppy; Lane 7; negative control (water).

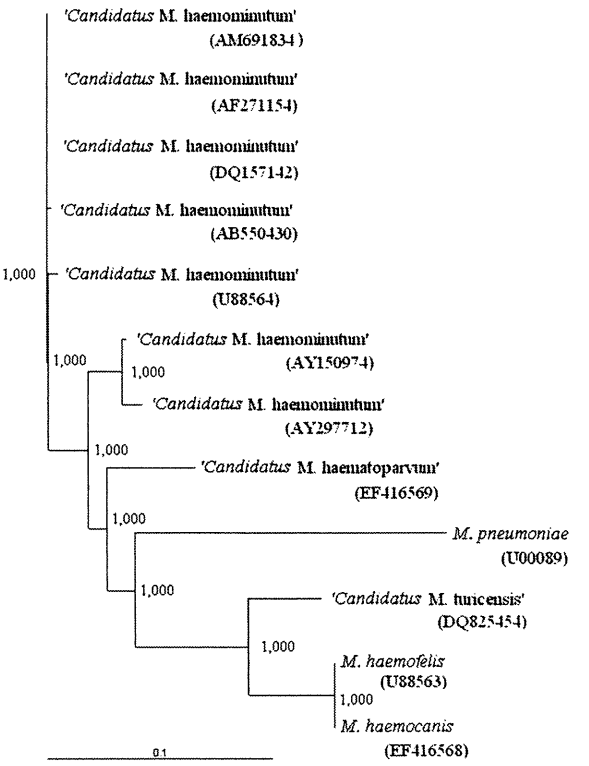

Fig. 2. Phylogenetic tree based on the 16S rRNA sequence comparison among feline and canine hemoplasmas. Genetic distances were computed with CLUSTAL W [14]. Hemoplasma sequences used in this analysis were as follows: '*Candidatus* M. haematoparvum' (EF416569), '*Candidatus* M. haemominutum '(AB550430, AF271154, AM691834, DQ157142, U88564, AY150974, AY297712), '*Candidatus* M. turicensis' (DQ825454), *M. haemocanis* (EF416568), and *M. haemofelis* (U88563). Out-group unit was M. pnemoniae (U00089). Numbers in the relevant branches refer to the values of boot-strap probability of 1,000 replications. Scale bar indicates the evolutionary distance value of 0.1 (a single nucleotide substitution per 10 nucleotides). AB550430 represents a hemoplasma strain detected from a dog (suffered from multi-centric lymphoma) in the present study.

evidence for direct transmission of hemoplasma in cat [24]. In dog, direct transmission of hemoplasmas is one the likely routes. There is also the possibility of transplacental infection [13]. Since we detected '*Candidatus* M. haemominutum' from the two puppies of three months old, there is another likely route of the vertical transmission of '*Candidatus* M. haemominutum' in dogs. The mechanisms of transmission of hemoplasma between dogs and cats have yet to be defined and need further exploration. Zhuang *et al.* [25] suggested the possibility that a dog was one of the hosts for the feline hemoplasma '*Candidatus* M. haemominutum'. However, it is likely that the presence of some underlying conditions (e.g., immunosuppressive, immature) may destroy the strict host specificity in mycoplasma infections, as previously reported in the cases of hemoplasma infection in human [3, 10, 11, 17]. Also, our results may indicate that dogs represent one of the hosts for the feline '*Candidatus* M. haemominutum'.

In conclusion, we first showed feline hemoplasma '*Candidatus* M. haemominutum' infected with dogs in Japan.

ACKNOWLEDGMENT. We thank Dr. Kou Chiba, the director of Will animal hospital, for the useful advice.

REFERENCES

1. Berent, L. M., Messick, J. B. and Cooper, S. K. 1998. Detection of *Haemobartonella felis* in cats with experimentally induced acute and chronic infections, using a polymerase chain reaction assay. *Am. J. Vet. Res.* **59**: 1215–1220.
2. Bobade, P. A., Nash, A. S. and Rogerson, P. 1988. Feline haemobartonellosis: clinical, haematological and pathological studies in natural infections and the relationship to infection with feline leukaemia virus. *Vet. Rec.* **122**: 32–36.
3. Duarte, M. I., Oliveira, M. S., Shikanai-Yasuda, M. A., Mariano, O. N., Takakura, C. F., Pagliari, C. and Corbett, C. E. 1992. Haemobartonella-like microorganism infection in AIDS patients: ultrastructural pathology. *J. Infect. Dis.* **165**: 976–977.
4. Flint, J. C., Roepke, M. H. and Jensen, R. 1959. Feline infections anemia. II. Experimental cases. *Am. J. Vet. Res.* **20**: 33–40.
5. Foley, J. E. and Pedersen, N. C. 2001. '*Candidatus* Mycoplasma haemominutum', a low-virulence epierythrocytic parasite of cats. *Int. J. Syst. Evol. Microbiol.* **51**: 815–817.
6. Fujihara, M., Watanabe, M., Yamada, T. and Harasawa, R. 2007. Occurrence of '*Candidatus* Mycoplasma turicensis' infection in domestic cats in Japan. *J. Vet. Med. Sci.* **69**: 1061–1063.
7. Harvey, J. W. 1998. pp. 166–171. *In*: Infectious Diseases of the Dog and Cat (Greene, C.E. ed.), WB Saunders, Philadelphia.
8. Hoskins, J. D. 1991. Canine haemobartonellosis, canine hepatozoonosis, and feline cytauxzoonosis. *Vet. Clin. North Am. Small Anim. Pract.* **21**: 129–140.
9. Hu, Z., Yin, J., Shen, K., Kang, W. and Chen, Q. 2009. Outbreaks of hemotrophic mycoplasma infections in China. *Emerg. Infect. Dis.* **15**: 1139–1140.
10. Kallick, C. A., Levin, S., Reddi, K. T. and Landau, W. L. 1972. Systemic lupus erythematosus associated with haemobartonella-like organisms. *Nat. New Biol.* **236**: 145–146.
11. Kallick, C. A., Thadhani, K. C. and Rice, T. W. 1980. Identification of Anaplasmataceae (Haemobartonella) antigen and antibodies in systemic lupus erythematosus. *Arthritis Rheum.* **23**: 197–205.
12. Kenny, M. J., Shaw, S. E., Beugnet, F. and Tasker, S. 2004. Demonstration of two distinct hemotropic mycoplasmas in French dogs. *J. Clin. Microbiol.* **42**: 5397–5399.
13. Krakowka, S. 1977. Transplacentally acquired microbial and parasitic diseases of dogs. *J. Am. Vet. Med. Assoc.* **171**: 750–753.
14. Lester, S. J., Hume, J. B. and Phipps, B. 1995. *Haemobartonella canis* infection following splenectomy and transfusion. *Can. Vet. J.* **36**: 444–445.
15. Messick, J. B. 2003. New perspectives about hemotrophic mycoplasma (formerly, *Haemobartonella* and *Eperythrozoon* species) infections in dogs and cats. *Vet. Clin. North Am. Small Anim. Pract.* **33**: 1453–1465.
16. Messick, J. B. 2004. Hemotrophic mycoplasmas (hemoplasmas): a review and new insights into pathogenic potential. *Vet. Clin. Pathol.* **33**: 2–13.
17. Santos, A. P., Santos, R. P., Biondo, A. W., Dora, J. M., Goldani, L. Z., de, Oliveira, S. T., de, Sa, Guimaraes, A. M., Timenetsky, J., de, Morais, H. A., Gonzalez, F. H. and Messick, J. B. 2008. Hemoplasma infection in HIV-positive patient, Brazil. *Emerg. Infect. Dis.* **14**: 1922–1924.
18. Sykes, J. E., Bailiff, N. L., Ball, L. M., Foreman, O., George, J. W. and Fry, M. M. 2004. Identification of a novel hemotropic mycoplasma in a splenectomized dog with hemic neoplasia. *J. Am. Vet. Med. Assoc.* **224**: 1946–1951, 1930–1931.
19. Sykes, J. E., Drazenovich, N. L., Ball, L. M. and Leutenegger, C. M. 2007. Use of conventional and real-time polymerase chain reaction to determine the epidemiology of hemoplasma infections in anemic and nonanemic cats. *J. Vet. Intern. Med.* **21**: 685–693.
20. Thompson, J. D., Higgins, D. G. and Gibson, T. J. 1994. CLUSTAL W: improving the sensitivity of progressive multiple sequence alignment through sequence weighting, position-specific gap penalties and weight matrix choice. *Nucleic Acids Res.* **22**: 4673–4680.
21. Watanabe, M., Hisasue, M., Souma, T., Ohshiro, S., Yamada, T. and Tsuchiya, R. 2008. Molecular detection of *Mycoplasma haemofelis* and '*Candidatus* Mycoplasma haemominutum' Infection in cats by direct PCR using whole blood without DNA extraction. *J. Vet. Med. Sci.* **70**: 1095–1099.
22. Wengi, N., Willi, B., Boretti, F. S., Cattori, V., Riond, B., Meli, M. L., Reusch, C. E., Lutz, H. and Hofmann-Lehmann, R. 2008. Real-time PCR-based prevalence study, infection follow-up and molecular characterization of canine hemotropic mycoplasmas. *Vet. Microbiol.* **126**: 132–141.
23. Westfall, D. S., Jensen, W. A., Reagan, W. J., Radecki, S. V. and Lappin, M. R. 2001. Inoculation of two genotypes of *Hemobartonella felis* (California and Ohio variants) to induce infection in cats and the response to treatment with azithromycin. *Am. J. Vet. Res.* **62**: 687–691.
24. Willi, B., Boretti, F. S., Tasker, S., Meli, M. L., Wengi, N., Reusch, C. E., Lutz, H. and Hofmann-Lehmann, R. 2007. From *Haemobartonella* to hemoplasma: molecular methods provide new insights. *Vet. Microbiol.* **125**: 197–209.
25. Zhuang, Q. J., Zhang, H. J., Lin, R. Q., Sun, M. F., Liang, X. J., Qin, X. W., Pu, W. J. and Zhu, X. Q. 2009. The occurrence of the feline "*Candidatus* Mycoplasma haemominutum" in dog in China confirmed by sequence-based analysis of ribosomal DNA. *Trop. Anim. Health Prod.* **41**: 689–692.

Journal of Virological Methods 174 (2011) 166–172

Contents lists available at ScienceDirect

Journal of Virological Methods

journal homepage: www.elsevier.com/locate/jviromet

Short communication

Species characterization in the genus *Pestivirus* according to palindromic nucleotide substitutions in the 5′-untranslated region

Massimo Giangaspero*, Ryô Harasawa

Veterinary Microbiology, School of Veterinary Medicine, Faculty of Agriculture, Iwate University, 18-8, Ueda 3 Chome, Morioka 020-8550, Iwate, Japan

Article history:
Received 23 April 2010
Received in revised form 25 March 2011
Accepted 5 April 2011
Available online 12 April 2011

Keywords:
Palindromic nucleotide substitutions
Pestivirus
Taxonomy
5′-UTR

A B S T R A C T

The palindromic nucleotide substitutions (PNS) at the three variable loci (V1, V2 and V3) in the 5′-untranslated region (UTR) of the *Pestivirus* genome have been considered for taxonomical segregation of the species, through the evaluation of 534 strains. On the basis of qualitative and quantitative secondary structure characteristics, species have been identified within the genus, determining genetic distances between species isolates, clarifying borderline and multirelated sequences, and characterizing and clustering the *Pestivirus* strains showing unexpected genomic sequences. Nine genomic groups have been identified: the species *Bovine viral diarrhea virus 1* (BVDV-1), *Bovine viral diarrhea virus 2* (BVDV-2), *Border disease virus* (BDV) and *Classical swine fever virus* (CSFV) and the tentative species Pronghorn, Giraffe, *Bovine viral diarrhea virus 3* (BVDV-3) (HoBi group), *Border disease virus 2* (BDV-2) (Italian small ruminant isolates) and Bungowannah.

Palindromic positions have been characterized according to changes in nucleotide base-pairs identifying low variable positions (LVP) including base-pairs present in less than 80% of the genus. The determination of divergence between single strain sequences or genetic groups was obtained easily by comparing base-pairing combinations from aligned secondary structures. This provided clear information such as the level of heterogeneity within a species, the relatedness between species, or facilitating the characterization and clustering of specific strains. The BVDV-1 and BDV species resulted heterogeneous, showing isolates located on a borderline in the species. Within the BVDV-2 species, two main genogroups were identified, with strains showing common sequence characteristics to both groups (multirelated strains). They could be allocated correctly by quantitative analysis. Similarly, the relation between CSFV and BDV species appeared very clearly. Also in this case, ambiguous strain sequences could be clustered in the species showing the lowest divergence values.

In conclusion, the proposed taxonomical procedure is based on the evaluation of only the strategic and highly conserved genome regions in the 5′-UTR. Furthermore, the application of quantitative analytical procedure allowed for a better determination of relation among species.

The genus *Pestivirus* of the family *Flaviviridae* is represented by four established species *Bovine viral diarrhea virus 1* (BVDV-1), *Bovine viral diarrhea virus 2* (BVDV-2), *Border disease virus* (BDV) and *Classical swine fever virus* (CSFV) and a tentative "Giraffe" species (Fauquet et al., 2005). These viruses infect a wide range of ungulate species like swine, cattle and sheep. They can cause prenatal and postnatal infections and heavy economical losses. Persistently infected animals are the main source of infection.

The pestiviruses were classified generally into different viral species according to their host origin: CSFV in pig, BVDV-1 and BVDV-2 in cattle, and BDV in sheep. However, cross infection may occur, thus, this approach resulted not sustainable. Therefore, isolates have to be classified according to their genetic sequence characteristics and the relatedness to viral strains that are used to define the type species. The Pestiviruses genome has a single-stranded, positive polarity RNA, composed by a sequence of about 12,500 nucleotides. It can be divided into three regions: a 5′-untranslated region (UTR), a single large open reading frame encoding a polyprotein, and a 3′-UTR. The virus-encoded polyprotein is cleaved into structural (C, Erns, E1 and E2) and non-structural proteins (Npro, P7, NS2-3, NS4A, NS4B, NS5A, NS5B). Previous reported phylogenetic analysis used different genomic regions, namely 5′-UTR, Npro or E2 genes, to distinguish genotypes within

* Corresponding author at: School of Veterinary Medicine, Faculty of Agriculture, Iwate University, 18-8, Ueda 3 Chome, Morioka 020-8550, Iwate, Japan.
Tel.: +81 196216158.
E-mail addresses: giangasp@iwate-u.ac.jp, giangasp@gmail.com (M. Giangaspero).

0166-0934/$ – see front matter © 2011 Elsevier B.V. All rights reserved.
doi:10.1016/j.jviromet.2011.04.004

Table 1
Summary of *Pestivirus* strains (*n* 534) evaluated according to the palindromic nucleotide substitution (PNS) method at the 5′-untranslated region of RNA.

Species	Number of strains	Host	Geographical origin
BVDV-1	274	Cattle, sheep, pig, deer, roe deer, human, contaminant	Argentina, Austria, Belgium, Brazil, Canada, China, Belgium, France, Germany, India, Ireland, Italy, Japan, New Zealand, Slovakia, South Africa, Spain, Sweden, Switzerland, UK, USA
BVDV-2	77	Cattle, sheep, contaminant	Argentina, Austria, Belgium, Brazil, Canada, France, Germany, Italy, Japan, Netherland, NewZealand, Slovakia, Tunisia, UK, USA
BVDV-3[a]	3	Cattle	Brazil, Thailand
BDV	131	Sheep, pyrenean chamois, cattle, pig, reindeer, wisent	Australia, France, Germany, Japan, New Zealand, Spain, Switzerland, Tunisia, Turkey, UK, USA
BDV-2[a]	3	Sheep, goat	Italy
CSFV	43	Pig, sheep	China, France, Garmany, Honduras, Italy, Japan, Malaysia, Netherlands, Poland, Russia, Spain, Switzerland, USA
Pronghorn[a]	1	Pronghorn	USA
Giraffe[a]	1	Giraffe	Kenya
Bungowannah[a]	1	Pig	Australia

[a] Tentative species.

each viral species. Npro refers to an N-terminal autoprotease that has no counterpart in other flaviviruses, whereas the E2 protein plays a major role in virus attachment and entry. In addition, E2 is also important for the induction of neutralizing antibodies. So far, genotyping using 5′-UTR, Npro or E2 sequences has given consistent results. As the 5′-UTR is relatively more conserved among all members within the genus, this genomic region was used to define pan-pestivirus reactive primers (Vilček et al., 1994), and was also more frequently utilised for the characterization of genotypes. Primary structure analysis, by sequence alignment and construction of phylogenetic trees, is the most common method for the classification of the virus isolates.

The nucleotide substitutions occurring at the level of the 5′-UTR genomic region are particularly important, since positive-sense RNA viruses include generally regulatory motifs, which are indispensable for viral survival. In Pestiviruses, the secondary structure of the 5′-UTR includes an internal ribosomal entry site (IRES), responsible for translational, transcriptional and replicational events (Deng and Brock, 1993). Thus, stable nucleotide variations at this level assume great importance in terms of virus evolutionary history. Nucleotide sequences at the variable loci, V1, V2 and V3, in the 5′-UTR of pestiviruses have been shown to be capable of forming a stable stem–loop structure peculiar to each *Pestivirus* species. The observation of nucleotide variations among virus strains at the level of the three specific variable loci in the secondary structure of the 5′-UTR has been conceived as a simple and practical procedure for genotyping (Harasawa and Giangaspero, 1998). The palindromic nucleotide substitutions (PNS) genotyping method has been further improved from the original concept limited to qualitative analysis (Giangaspero and Harasawa, 2007), allowing the taxonomical segregation of the genus *Pestivirus* into six species: BVDV-1, BVDV-2, CSFV, BDV, the tentative species Giraffe and a new proposed taxon named Pronghorn.

The relatively large number of new deposited sequences of isolates from domestic and wild animals and the recent evidence of novel "atypical" *Pestivirus* sequences, as for example the strains D32/00_'HoBi' (Schirrmeier et al., 2004) and Th/04_KhonKaen (Liu et al., 2009a) isolated in cattle infected naturally, in Brazil and Thailand, respectively, or the Bungowannah virus isolated from piglets in Australia (Kirkland et al., 2007), motivated the necessity for a updated application of the PNS method.

Qualitative and quantitative evaluation of genomic sequence divergence, in terms of palindromic nucleotide base pairings variations, has been applied for taxonomical segregation of species, through the evaluation of 534 genomic sequences. The nucleotide sequences in the 5′-UTR of *Pestivirus* strains, with different geographical origins, from different host species or contaminants of biological products, were obtained from the GenBank DNA database, provided by authors or obtained in our laboratories (Table 1) (detailed list of analysed strains available under request).

Nucleotide sequence secondary structures were predicted according to the algorithm of Zuker and Stiegler (1981) using the Genetyx-Mac version 10.1 program package (Software Development Co., Ltd., Tokyo, Japan). The minimum free energy was calculated by the method of Freier et al. (1986). Relevant secondary structure regions in the 5′-UTR were used for genotyping based on the palindromic nucleotide substitutions method (Harasawa and Giangaspero, 1998; Giangaspero and Harasawa, 2007). The identification of species within the genus has been achieved according to highly conserved base pairs in the three variable palindromic loci, based on a series of specific passages focused on the qualitative and quantitative analysis of the secondary structures of the strains in the genus. The first step was qualitative and consisted in the characterization of the different positions of the 3 stems and loops in the 5′-UTR sequences of all the considered strains belonging to the genus. Variable loci were positioned in the prototype *Pestivirus* strain BVDV-1 Osloss sequence (De Moerlooze et al., 1993) as follows: V1 197-235, V2 267-289 and V3 293-311. Only V2 locus was composed by a constant number of nucleotides (*n* 23). The variation of loops in V1 and V3 loci determined difference in size of palindromes. Secondary structure sequences showing divergent base pair combinations have been aligned for comparison. For strain comparison, differences in number and type of nucleotides constituting the palindromes have been considered (Giangaspero and Harasawa, 2007). Palindromic positions have been characterized according to changes in nucleotide base pairs identifying low variable positions (LVP) including base pairs present in less than 80% in the genus, thus, selecting specific base pairings suitable for genus and species determination. The second step was quantitative, allowing the identification of genomic groups among *Pestivirus* strains by clustering the base pair combinations according to LVP. Cross comparisons between types within the genus have been evaluated by computing the divergence percentage, identifying strains showing multirelation or borderlines, and quantifying the heterogeneity of a species and the genetic distance between species in terms of variation of base pairs in the secondary structure (Table 3).

The observation made on the nucleotide sequences of the three variable loci at the level of the 5′-UTR genomic region of *Pes-*

Table 2
Palindromic nucleotide substitutions (PNS) characteristic to the genus *Pestivirus*. The position of base pairings is defined by numbering from the bottom of the variable locus.

	Locus	Characteristic PNS markers
Genus		
	V1	Absence in position 22—size of V1 21 bp (exception U); C C bulge in position 11; A-U in position 10; C-G in position 8 (exceptions U*G, U-A and G G bulge); U-A in position 7 (exception G-C and A A bulge); A in position 6 (exception G); U*G in position 5; U in position 5 right nucleotide; G-C in position 4.
	V2	GGGGU loop (exception GGGGC); C-G in position 8 (exception U*G).
Species		
BVDV-1	V1	U-A in position 15 (exception U*G or C-G);
	V2	G-C in position 5 (exception A-U);
	V3	G-C in position 5; A in position 10 (exceptions R:H).
BVDV-2	V1	A-U or A C bulge in position 20 (exceptions Z:H); A,G or U in position 21 (exception GG);
	V2	U-A or U*G in position 6 (exception C A bulge);
	V3	A-U or A C bulge in position 7 (exception G-C).
BVDV-3 tentative species (HoBi group)	V1	U-A in position 15;
	V3	G-C or G*U in position 3; A-U or G-C in position 7; A in position 10.
BDV	V1	G-C or A-U in position 15 (exceptions C U and A C bulges);
	V3	U C and U U bulges or U*G in position 7 (exceptions A-U, U-A and C C, A C, C U and C A bulges).
BDV-2 tentative species (Italian ovine isolates)	V1	U-A or C A bulge in position 15;
	V3	G*U or G G bulge in position 8.
CSFV	V1	U-A in position 13 (exception U*G);
	V3	U-A in position 2; U or C in position 8 (exception A).
Pronghorn tentative species	V1	G-C in position 2; U-A in position 9; U-A in position 12; U-A in position 15;
	V2	G-C in position 4;
	V3	G A bulge in position 5.
Giraffe tentative species	V1	C-G in position 2; U*G in position 20;
	V2	C-G in position 7;
	V3	C-G in position 4; G*U in position 7.
Bungowannah tentative species	V1	A-U in position 2; G-C in position 7; U-A in position 9; U-A in position 12; G-C in position 13;
	V2	A-U in position 3; G-C in position 4;
	V3	U-A in position 4; G A bulge in position 10; A in position 11.

Table 3
Identified species within genus *Pestivirus*.

(A) Relations within species

Species	Divergence within genus	Divergence within species %/mean value	Multirelated strains	Borderline strains
BVDV-1	0.33	6.43/9.54	None	3186V6, J, R, S, MV98CB95, W, ZM-95
BVDV-2	2.00	11.15/7.89	None	None
BVDV-2A	1.93	0.40/5.37	vs 2B 713-2, 5521-95, BSE1239, UVR420, 97/730	
BVDV-2B	2.25	0/7.28	vs 2A VS-123.4, VS-63	
BVDV-3	2.00	0/4	None	None
BDV	2.22	27.89/11.22	vs CSFV 91-F-6731, 91-F-6732	Aydin/04-TR, Burdur/05-TR
BDV-2	2.33	0/4.5	None	None
CSFV	2.33	0/5.52	vs BDV Kanagawa/74	None
Pronghorn	4	0/0	None	None
Giraffe	7	0/0	None	None
Bungowannah	7	0/0	None	None

(B) Relations among species

Species	Divergence %/divergence value mean									
BVDV-2	100/19.53									
BVDV-2A	100/19.78									
BVDV-2B	100/18.54		33.20/12.85							
BVDV-3	100/16.94	100/17.10	100/17.02	100/17.41						
BDV	100/19.70	100/18.73	100/18.57	100/19.38	100/18.83					
BDV-2	99.62/17.86	100/17.79	100/17.71	100/18.08	100/19.33	97.74/16.30				
CSFV	100/19.29	100/20.68	100/20.63	100/20.88	100/19.51	69.30/14.48	100/17.13			
Pronghorn	100/19.43	100/21.02	100/20.64	100/22.50	100/19.00	100/20.39	100/17.00	100/21.83		
Giraffe	100/26.00	100/20.17	100/19.84	100/21.50	100/23.33	100/21.66	100/20.33	100/23.38	100/22.00	
Bungowannah	100/24.23	100/26.07	100/26.15	100/25.75	100/25.00	100/25.98	100/24.66	100/24.05	100/22.00	100/30.00
	BVDV-1	BVDV-2	BVDV-2A	BVDV-2B	BVDV-3	BDV	BDV-2	CSFV	Pronghorn	Giraffe

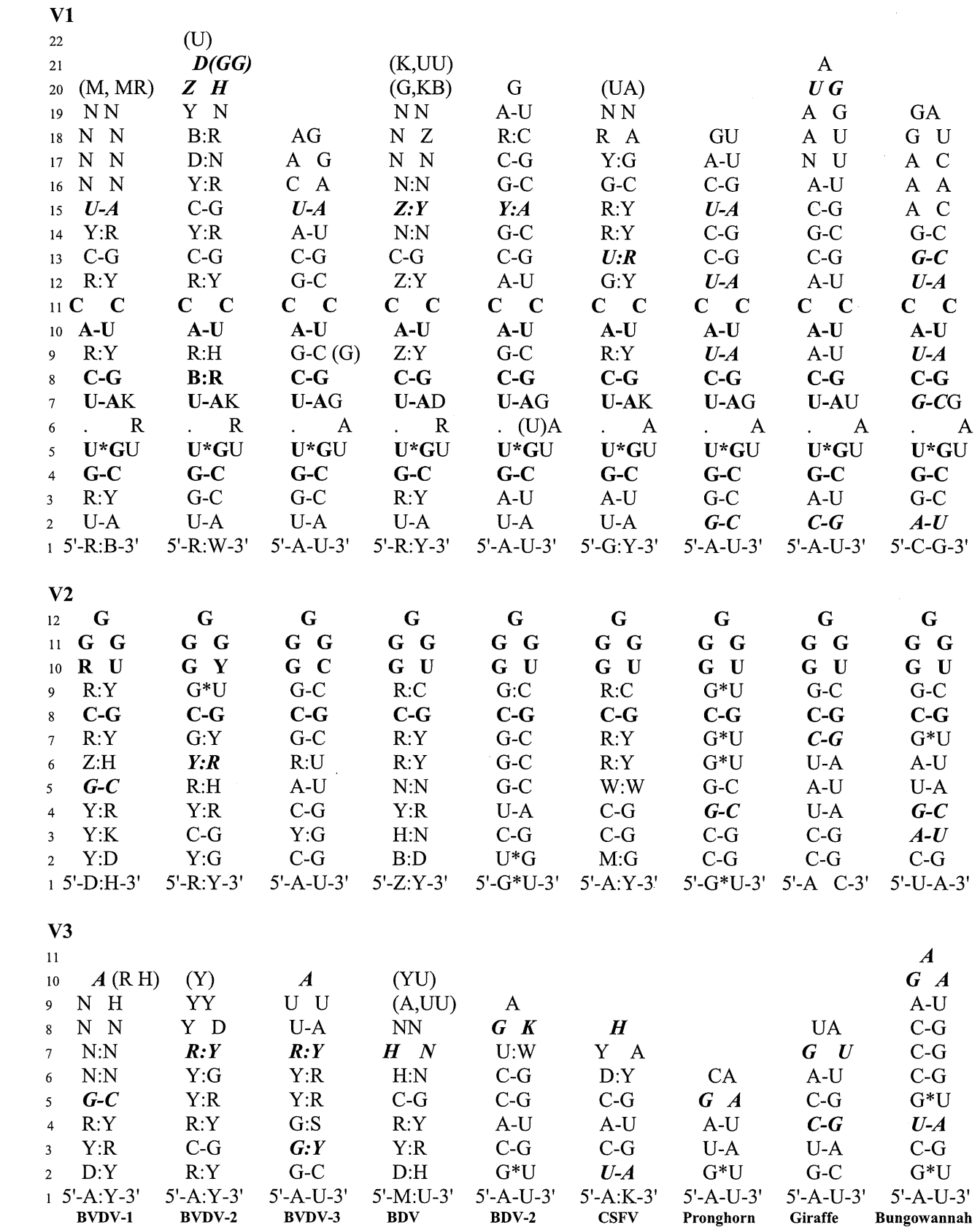

Fig. 1. V1–V3 palindromic loci in the 5′-UTR of the genus *Pestivirus* species. Base pairings characteristic to the genus (PNS genus specific) are shown in bold. The characteristic base pairings of the species BVDV-1, BVDV 2, BDV, CSFV, and the new proposed taxons BVDV-3, BDV-2, Giraffe, Pronghorn and Bungowannah (PNS species specific) are represented in bold and italic. The position of base-pairings is defined by numbering from the bottom of the secondary structures. Watson–Crick base pairings are indicated by a dash (-); tolerated pairings in secondary structure are indicated by an asterisk (*); interchangeable base pairings are indicated by a column (:). M = A or C; R = A or G; W = A or U; S = C or G; Y = C or U; K = G or U; Z = A or C or G; H = A or C or U; D = A or G or U; B = C or G or U; N = A or C or G or U.

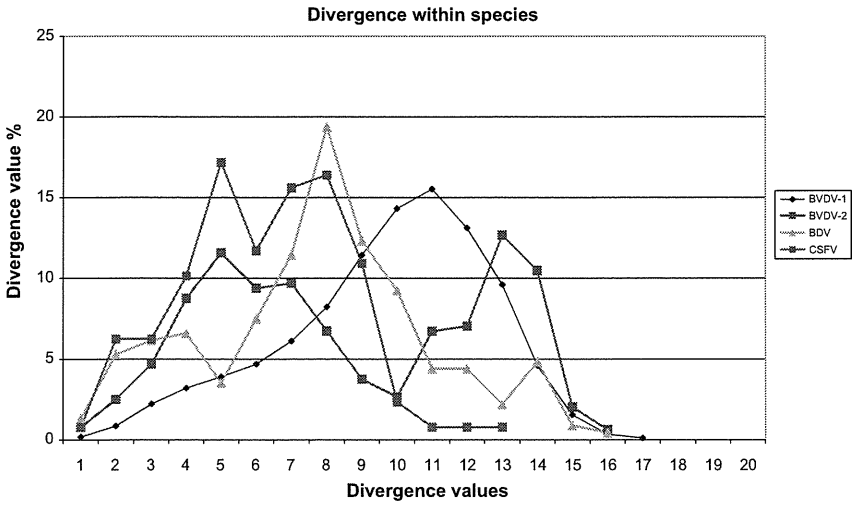

Fig. 2. Determination of the level of heterogeneity within the single species in the genus *Pestivirus* (PNS method). The divergence values between single strain sequences were obtained by comparing base pairing from aligned secondary structure sequences, helping for the characterization and clustering of specific strains. Species divergence limit value was 13. Within the BVDV-2 species, heterogeneity was particularly marked, represented graphically by a curve characterized by two distinct peaks. The left peak (low divergence values) was related to homogeneity within groups. Comparison of homogeneous groups resulted in higher divergence values (right peak), indicating clear divergence between the groups. This corresponded to two identifiable main genogroups: BVDV-2A, characterized by a cosmopolitan diffusion, and BVDV-2B, restricted to South America. In both groups, some strains showed common sequence characteristics to both groups (multirelated strains). They could be allocated correctly by quantitative analysis.

tivirus strains, according to the PNS genotyping method, allowed to the identification of consensus motifs shared by all the *Pestivirus* species, genus specific base-pairings positioned in the V1 and V2 loci, and characteristic species specific PNS, respectively (Table 2). On the base of qualitative and quantitative secondary structure characteristics, nine species have been identified: *Bovine viral diarrhea virus 1* (BVDV-1), *Bovine viral diarrhea virus 2* (BVDV-2), *Classical swine fever virus* (CSFV), *Border disease virus* (BDV), and the tentative species Pronghorn, Giraffe, *Bovine viral diarrhea virus 3* (BVDV-3) (HoBi group), *Border disease virus 2* (BDV-2) (Italian small ruminant isolates) and Bungowannah. The secondary structure variable loci in the 5′-UTR of the *Pestivirus* species are reported in Fig. 1. The genetic markers useful for taxonomic purposes identified at genus level were represented by base pairings from highly conserved, homogeneous positions. At species level, characteristic base pairings determinative for species identification (species determinative at genus level (SDG) not shared with other species) were identified from conserved positions only in BVDV-3, Pronghorn, Giraffe and Bungowannah species. However, clear identification for BVDV-1, BVDV-2, BDV, BDV-2 and CSFV species was obtained using specific combinations of base-pairings in the sequence (species determinative (SD) from conserved positions species specific, shared with other species). These base-pairings acquired significance only when combined, and they were non specific when considered separately.

The palindromic structures were identifiable in linear sequences. However, it was easier to find them observing the secondary structure. The evaluation of the secondary structure based on a qualitative observation of the nucleotide variations was supported and confirmed through the application of a quantitative approach. The determination of divergence between single strain sequences or genetic groups was obtained easily by comparing base pairing from aligned secondary structure sequences. This provided clear information such as the level of heterogeneity within a species, the genetic distance between species in terms of variation of base pairs in the secondary structure, or helping for the characterization and clustering of specific strains (Table 3). The BVDV-1 and BDV species resulted heterogeneous, showing borderline strain sequences. Strains 3186V6, J, R, S, W (Vilček et al., 2001), and MV98CB95 (Baule et al., 1997) isolated from cattle, and the pig strain ZM-95 (Xu et al., 2006) were located on a borderline in the BVDV-1 species. Their sequences showed qualitative similarities with the BVDV-1 species, sharing partially the specific PNS species markers, but with high divergence values, thus, candidates for reclustering as separate groups in the genus. Similarly, the strains Aydin/04-TR and Burdur/05-TR (Oguzoglu et al., 2009), isolated from sheep in Turkey, showing partial genetic relatedness only with members of the BDV species, were clustered in the species as borderline. Within the BVDV-2 species, heterogeneity was particularly marked, represented graphically by a curve characterized by two distinct peaks (Fig. 2). The left peak (low divergence values) was related to homogeneity within groups. Comparison of homogeneous groups resulted in higher divergence values (right peak), indicating clear divergence between the groups. However, mean divergence value (12.85) did not allowed their segregation into different species. This corresponded to two identifiable main genogroups: BVDV-2A, characterized by a cosmopolitan diffusion, and BVDV-2B, restricted to South America. In both groups, some strains showed common sequence characteristics to both groups (multirelated strains). They could be allocated correctly by quantitative analysis. Similarly, the relation between CSFV and BDV species appeared very clearly (Fig. 3), as example of the genetic relatedness determination among *Pestivirus* species. The computing of the divergence by comparing sequences from both species showed very low values (mean 14.48) when compared to those obtained with other *Pestivirus* species (from 17 and 17.13 with Pronghorn and BDV-2, to 24.05 with Bungowannah) (Table 3). Also in this case, ambiguous strains, sharing common sequence characteristics to both species (multirelated strains), could be clustered in the species showing the lowest divergence values.

The classification among *Pestivirus* species strains according to PNS analysis based on changes in the secondary structure was compared with those based on the 5′-UTR primary structure, carried out through alignment and construction of phylogenetic trees. The results were generally comparable. In particular, new taxons have been defined due to specific base-pairings, despite the limited number of allocated strains. This corresponded to the observations made by different investigators, evaluating the 5′-UTR or other genomic regions (Schirrmeier et al., 2004; Vilček et al., 2005; Cortez et al., 2006; Kirkland et al., 2007). However, some atypical strains were

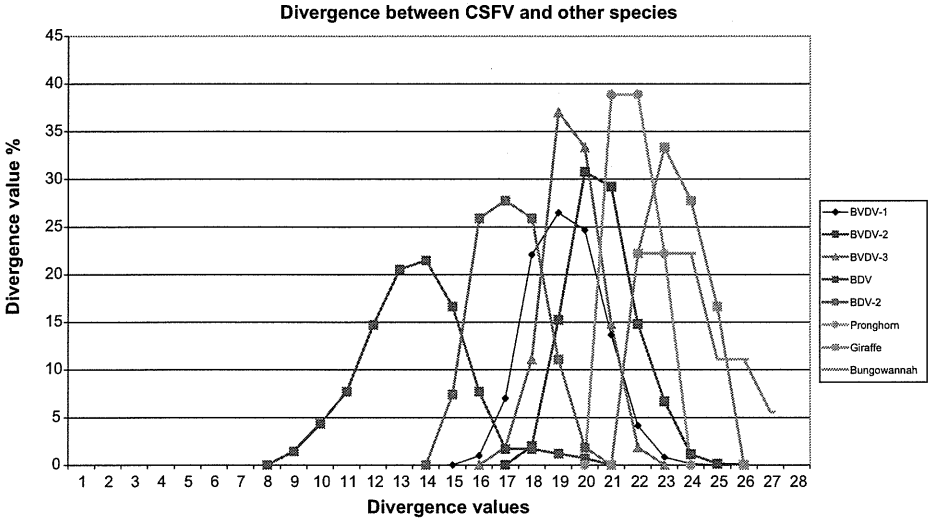

Fig. 3. Determination of the genetic relatedness among *Pestivirus* species (PNS method). The comparison of CSFV strain 5′-UTR sequences with those from other species showed a very clear relation between CSFV and BDV species, with very low divergence values (mean 14.48). Ambiguous strains, sharing common sequence characteristics to both species (multirelated strains), could be clustered in the species showing the lowest divergence values.

related to controversial taxonomical clustering, in particular for sequences isolated from small ruminants. The sheep isolates from Tunisia (strains 33S, 35, 35T, Lot21, SN1T, SN3G, SN2T, 37A, RM and BM01 isolate 5), reported by Thabti et al. (2005), associated to clinical cases due to the use of a vaccine produced on contaminated cell lines derived from ovine, and natural infections, represented an interesting pestivirus intermediate group, genetically close to CSFV but antigenically related to BDV. They have been reported by the author as members of a new genotype of the BDV species. Two French ovine isolates, 91-F-6731 and 91-F-6732 (Dubois et al., 2008), showed high genetic similarity with the Tunisian strains. The author indicated that both group of strains belong to a novel species named Tunisian. Other studies reported the Tunisian strains as a separate species (Valdazo-Gonzalez et al., 2006, 2007; Liu et al., 2009b), or belonging to the BDV species (De Mia et al., 2005). The application of PNS segregated these isolates in the BDV species, based on the divergence values when compared to CSFV and BDV sequences, despite the sharing of CSFV specific base pairing U-A in position 2 in V3. In particular, the Tunisian and French isolates constituted a homogeneous group with divergence mean of 5.5 within the group. The strains showed lower divergence values with BDV than with CSFV, mean 12.07 and 12.72, respectively. Furthermore, the strains 712/02 (De Mia et al., 2005), LA/91/05 (Giammarioli et al., unpublished) and TO/121/04 (De Mia, unpublished) isolated from small ruminants in Italy, and reported as genotype of BDV species, have been clustered as new taxon in the genus *Pestivirus*, showing a divergence value mean of 16.30 with the BDV species. The ovine strains 098, 119 and 63 from Tunisia (Thabti et al., unpublished) have been clustered within the BVDV-2 species, group BVDV-2A, constituting a separate genotype in addition to the four genotypes, BVDV-2a, BVDV-2b, BVDV-2c, and BVDV-2d previously described (Giangaspero et al., 2008a). In the present study, the nomenclature of HoBi group isolates as BVDV-3, proposed by Liu et al. (2009b), was adopted in reason to the close relation with the BVDV-1 species.

Problematic sequences showing difficulties for clustering based on primary structure analysis highlight the interest of applying PNS in order to clarify possible taxonomical discrepancies. However, as disadvantage, apart the lack of current informatics design of the method, only 5′-UTR is targeted and it is not applicable a combined study approach on different portions of the genome such as Npro, since no other genomic regions have been explored for the application of PNS.

The PNS demonstrated to offer a reliable alternative for viral investigations to classical taxonomical methods based on primary sequence structure. As secondary structures are essential for survival of the viral population, variations in the involved genomic regions might be related with biological characteristics, which in turn might correlate with classification. The relevant role of the 5′-UTR in the translational, transcriptional and replicational mechanisms in pestiviruses implies that its secondary structures (e.g. palindromic structures) must be highly conserved, and that observed mutations are particularly meaningful. Since these mutations are observed as conserved nucleotide changes, they may be considered as the occurrence of a micro evolution step through selection in the phylogenetic history of the virus. On the base of the above mentioned considerations the nucleotide substitutions at the level of the palindromic structures in the genomic 5′-UTR may represent a useful genetic marker for taxonomical procedures in pestiviruses and theoretically for other RNA positive strand viruses. Secondary structures predicted at the variable regions in the 5′-UTR showed typical PNS which were useful for classification or genotyping of hepatitis C virus (Giangaspero et al., 2008b).

In conclusion, the proposed method provides results comparable with other taxonomical procedures based on 5′-UTR primary structure evaluation, but it differs from them in that only the strategic and highly conserved genome regions in the 5′-UTR, and therefore the most meaningful nucleotide sequences at this level, are considered. Thus accurate parameters for species identification in terms of nucleotide sequence homology are made available with great advantage for simplification of virological investigations. Furthermore, the application of quantitative analytical procedure allowed to a better determination of relation among species and genotypes. *Pestivirus* strains showing unexpected genomic sequences such as Giraffe (Plowright, 1969), Wisent Casimir (Becher et al., 1999), Chamois-1 (Arnal et al., 2004), Pronghorn (Vilček et al., 2005), HoBi group strains (Schirrmeier et al., 2004; Cortez et al., 2006; Liu et al., 2009a) and Bungowannah (Kirkland et al., 2007) have been characterized easily and clustered within the genus by PNS method. The procedures require constant adaptability to eventual new and different observations. In addition, further investigations will possibly provide new variants in the species and other genotypes or subtypes might be characterized, requiring subsequent revision of identification markers. Nevertheless, the manual searching of relevant base-pairings and direct observation of the sequences still remain the method's main

limitations. Further efforts are required in order to develop the PNS method in a fully computerized procedure for easy user-access and rapid testing with reliable results.

References

Arnal, M., Fernandez-de-Luco, D., Riba, L., Maley, M., Gilray, J., Willoughby, K., Vilček, S., Nettleton, P., 2004. A novel pestivirus associated with deaths in Pyrenean chamois (*Rupicapra pyrenaica pyrenaica*). J. Gen. Virol. 85, 3653–3657.

Baule, C., van Vuuren, M., Lowings, J.P., Belak, S., 1997. Genetic heterogeneity of bovine viral diarrhoea viruses isolated in Southern Africa. Virus Res. 52 (2), 205–220.

Becher, P., Orlich, M., Kosmidou, M., Baroth, M., Thiel, J.-H., 1999. Genetic diversity of pestiviruses: identification of novel groups and implications for classification. Virology 262, 64–71.

Cortez, A., Heinemann, M.B., de Castro, A.M.M.G., Soares, R.M., Pinto, A.M.V., Alfieri, A.A., Flores, E.F., Leite, R.C., Richtzenhain, L.J., 2006. Genetic characterization of Brazilian bovine viral diarrhea virus isolates by partial nucleotide sequencing of the 5′-UTR region. Pesqui. Vet. Bras. 26 (4), 211–216.

De Mia, G.M., Greiser-Wilke, I., Feliziani, F., Giammarioli, M., De Giuseppe, A., 2005. Genetic characterization of a caprine pestivirus as the first member of a putative novel pestivirus subgroup. J. Vet. Med. B Infect. Dis. Vet. Public Health 52 (5), 206–210.

De Moerlooze, L., Lecomte, C., Brown-Shimmer, S., Schmetz, D., Guiot, C., Vandenbergh, D., Allaer, D., Rossius, M., Chappuis, G., Dina, D., Renard, A., Martial, J.A., 1993. Nucleotide sequence of the bovine viral diarrhoea virus Osloss strain: comparison with related viruses and identification of specific DNA probes in the 5′ untranslated region. J. Gen. Virol. 74, 1433–1438.

Deng, R., Brock, K.V., 1993. 5′ and 3′ untranslated regions of pestivirus genome: primary and secondary structure analyses. Nucleic Acids Res. 21, 1949–1957.

Dubois, E., Russo, P., Prigent, M., Thiéry, R., 2008. Genetic characterization of ovine pestiviruses isolated in France, between 1985 and 2006. Vet. Microbiol. 130, 69–79.

Fauquet, C.M., Mayo, M.A., Maniiloff, J., Desselberger, U., Ball, L.A., 2005. Virus Taxonomy. Classification and Nomenclature of Viruses. Elsevier, Academic Press, San Diego.

Freier, S.M., Kierzek, R., Jaeger, J.A., et al., 1986. Improved free-energy parameters for predictions of RNA duplex stability. Proc. Natl. Acad. Sci. U.S.A. 83, 9373–9377.

Giangaspero, M., Harasawa, R., 2007. Numerical taxonomy of genus *Pestivirus* based on palindromic nucleotide substitutions in the 5′ untranslated region. J. Virol. Methods 146, 375–388.

Giangaspero, M., Harasawa, R., Weber, E.L., Belloli, A., 2008a. Genoepidemiological evaluation of Bovine viral diarrhea virus 2 species based on secondary structures in the 5′ genomic untranslated region. J. Vet. Med. Sci. 70 (6), 571–580.

Giangaspero, M., Harasawa, R., Zanetti, A., 2008b. Taxonomy of Genus *Hepacivirus*. Application of palindromic nucleotide substitutions for the determination of genotypes of human hepatitis C virus species. J. Virol. Methods 153, 280–299.

Harasawa, R., Giangaspero, M., 1998. A novel method for pestivirus genotyping based on palindromic nucleotide substitutions in the 5′-untranslated region. J. Virol. Methods 70, 225–230.

Kirkland, P.D., Frost, M.J., Finlaison, D.S., King, K.R., Ridpath, J.F., Gu, X., 2007. Identification of a novel virus in pigs-Bungowannah virus: a possible new species of pestivirus. Virus Res. 129 (1), 26–34.

Liu, L., Kampa, J., Belák, S., Baule, C., 2009a. Virus recovery and full-length sequence analysis of atypical bovine pestivirus Th/04_KhonKaen. Vet. Microbiol. 138, 62–68.

Liu, L., Xia, H., Wahlberg, N., Belák, S., Baule, C., 2009b. Phylogeny, classification and evolutionary insights into pestiviruses. Virology 385, 351–357.

Oguzoglu, T.C., Tan, M.T., Toplu, N., Demir, A.B., Bilge-Dagalp, S., Karaoglu, T., Ozkul, A., Alkan, F., Burgu, I., Haas, L., Greiser-Wilke, I., 2009. Border disease virus (BDV) infections of small ruminants in Turkey: a new BDV subgroup? Vet. Microbiol. 135, 374–379.

Plowright, W., 1969. Other virus diseases in relation to the JP15 programme. In: Joint Campaign Against Rinderpest. Proceedings of the 1st technical review meeting, phase IV, Mogadiscio , Organization of African Unity, Kenya, pp. 19–23.

Schirrmeier, H., Strebelow, G., Depner, K., Hoffmann, B., Beer, M., 2004. Genetic and antigenic characterization of an atypical pestivirus isolate, a putative member of a novel pestivirus species. J. Gen. Virol. 85 (12), 3647–3652.

Thabti, F., Letellier, C., Hammami, S., Pepin, M., Ribiere, M., Mesplede, A., Kerkhofs, P., Russo, P., 2005. Detection of a novel border disease virus subgroup in Tunisian sheep. Arch. Virol. 150 (2), 215–229.

Valdazo-Gonzalez, B., Alvarez-Martinez, M., Greiser-Wilke, I., 2006. Genetic typing and prevalence of Border disease virus (BDV) in small ruminant flocks in Spain. Vet. Microbiol. 117 (2–4), 141–153.

Valdazo-Gonzalez, B., Alvarez-Martinez, M., Sandvik, T., 2007. Genetic and antigenic typing of border disease virus isolates in sheep from the Iberian Peninsula. Vet. J. 174 (2), 316–324.

Vilček, S., Herring, J.A., Nettleton, P.F., Lowings, J.P., Paton, D.J., 1994. Pestiviruses isolated from pigs, cattle and sheep can be allocated into at least three genogroups using polymerase chain reaction and restriction endonuclease analysis. Arch. Virol. 136, 309–323.

Vilček, S., Paton, D.J., Durkovic, B., Strojny, L., Ibata, G., Moussa, A., Loitsch, A., Rossmanith, W., Vega, S., Scicluna, M., Palfi, V., 2001. Bovine viral diarrhoea virus genotype 1 can be separated into at least eleven genetic groups. Arch. Virol. 146, 99–115.

Vilček, S., Ridpath, J.F., Van Campen, H., Cavender, J.L., Warg, J., 2005. Characterization of a novel pestivirus originating from a Pronghorn antilop. Virus Res. 108, 187–193.

Xu, X., Zhang, Q., Yu, X., Liang, L., Xiao, C., Xiang, H., Tu, C., 2006. Sequencing and comparative analysis of a pig bovine viral diarrhea virus genome. Virus Res. 122 (1–2), 164–170.

Zuker, M., Stiegler, P., 1981. Optimal computer folding of large RNA sequences using thermodynamics and auxiliary. Nucleic Acids Res. 9, 133–148.

NOTE *Bacteriology*

Molecular Identification of '*Candidatus* Mycoplasma haemovis' in Sheep with Hemolytic Anemia

Jin SUZUKI[1)], Fumina SASAOKA[1)], Masatoshi FUJIHARA[1)], Yusaku WATANABE[1)], Tomoko TASAKI[2)], Shinichi ODA[2)], Saori KOBAYASHI[3)], Reeko SATO[3)], Kazuya NAGAI[4)] and Ryô HARASAWA[1)]*

Departments of [1)]Veterinary Microbiology, [2)]Animal Science, [3)]Veterinary Internal Medicine and [4)]Cryobiofrontier Research Center, Faculty of Agriculture, Iwate University, Morioka 020–8550, Japan

(Received 10 March 2011/Accepted 12 April 2011/Published online in J-STAGE 26 April 2011)

ABSTRACT. We examined the presence of hemoplasmas, hemotropic mycoplasmas, among 11 sheep (*Ovis aries*) with regenerative and hemolytic anemia and found six of them were positive by real-time PCR. The positive samples were then subjected to conventional PCR for direct sequencing of the 16S rRNA gene. Nucleotide sequences of all the positive samples were identified as the 16S rRNA gene of '*Candidatus* Mycoplasma haemovis' by phylogenetic analysis, demonstrating the infections with this particular hemoplasma species in Japan.

KEY WORDS: hemoplasma, mycoplasma, ovine, rRNA, sheep.

J. Vet. Med. Sci. 73(8): 1113–1115, 2011

Hemoplasmas are tiny epierythrocytic prokaryotes that lack a cell wall like other mycoplasmas and are susceptible to tetracyclines, but have never been cultured *in vitro*. Infections may lead to hemolytic anemia in animals, but veterinary investigation had been hampered by the lack of appropriate diagnostic procedures. Although most studies relied on cytological identification of the organisms on blood smears, this method has a low diagnostic sensitivity and cannot differentiate the species [4]. Besides, this diagnostic method may misidentify the hemoplasmas as Howell-Jolly bodies, since the both appear frequently after splenectomy, associate with anemia, and contain DNA. Currently only two hemoplasma species, *Mycoplasma ovis* (previously known as *Eperythrozoon ovis*) [5] and '*Candidatus* Mycoplasma haemovis' [3] are recognized in sheep (*Ovis aries*). Although *M. ovis* infection among sheep is prevalent throughout the world, '*Candidatus* M. haemovis' has not been detected in Japan so far. In the present study we investigated an outbreak of infection with '*Candidatus* M. haemovis' in anemic sheep on an experimental farm in Iwate University, Morioka (latitude 39.7N and longitude 141.1E), Japan.

The disease manifested between October and December of 2010, and mainly affected yearlings, which were purchased from a commercial farm in the Iwate prefecture. Hematological examination was carried out on 11 animals with mild regenerative anemia and blood smears were prepared for Giemsa staining. Small, coccoid, epicellular parasites were detected on erythocytes by microscopic examination of the Giemsa-stained blood smears (Fig. 1). Hematocrit, hemoglobin, and red blood cells values of these animals were 9.6 to 25.7%, 2.5 to 7.1 g/d*l*, and 350 to 800 × 10^4/d*l*, respectively, being below the normal ranges.

Total DNA was extracted from 200 μl EDTA-anticoagulated blood samples collected from sheep using the QIAamp DNA Blood Mini Kit (Qiagen, Hilden, Germany) according to the manufacturer's instructions. Negative controls consisting of 200 μl phosphate-buffered saline were prepared with each batch. Extracted DNA samples were stored at –20°C prior to use. To detect the hemoplasmas in real-time PCR, specific primers for the 16S rRNA gene were originally designed. Forward primer Hemo-F, 5'-TCCATA TTCCTACGGGAAGCAA-3', and reverse primer Hemo-R, 5'-TACCCCTTGATTAACTCTAA-3'. Real-time PCR was performed in a SmartCycler instrument (Cepheid, Sunnyvale, CA, U.S.A.) with SYBR Premix Ex *Taq* (Code #RR041A, TaKaRa Bio, Shiga, Japan). The reaction mixture contained 1 μl of each primer (10 pmol/μl), 12.5 μl of

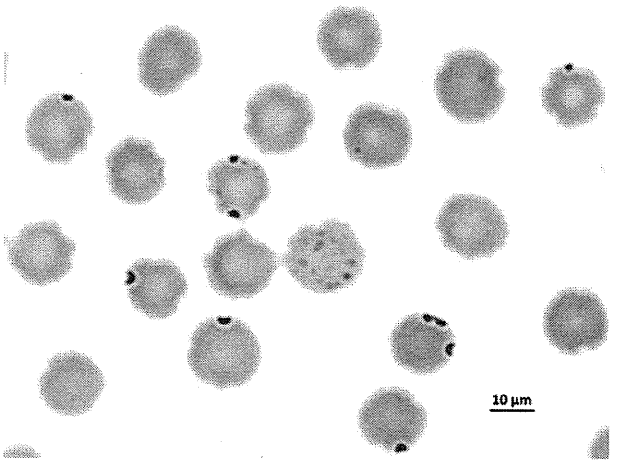

Fig. 1. Giemsa-stained blood smear from an affected sheep with '*Candidatus* M. haemovis'. Hemotrophic mycoplasma cells were seen on the surface of erythrocytes.

* CORRESPONDENCE TO: HARASAWA, R., Department of Veterinary Microbiology, Faculty of Agriculture, Iwate University, Morioka 020–8550, Japan.
e-mail: harasawa-tky@umin.ac.jp